NUMERICAL METHODS FOR NONLOCAL PROBLEMS

A Dissertation Submitted to
the Graduate School of Engineering and Sciences of
İzmir Institute of Technology
in Partial Fulfillment of the Requirements for the Degree of

DOCTOR OF PHILOSOPHY

in Mathematics

by
Adem KAYA

July 2018
İZMİR

We approve the thesis of **Adem KAYA**

Examining Committee Members:

Prof. Dr. Gamze TANOĞLU
Department of Mathematics, İzmir Institute of Technology

Prof. Dr. İsmail ASLAN
Department of Mathematics, İzmir Institute of Technology

Prof. Dr. Emine MISIRLI
Department of Mathematics, Ege University

Asst. Prof. Dr. Olha Ivanyshyn YAMAN
Department of Mathematics, İzmir Institute of Technology

Asst. Prof. Dr. Sevin GÜMGÜM
Department of Mathematics, İzmir University of Economics

6 July 2018

Prof. Dr. Gamze TANOĞLU
Supervisor, Department of Mathematics
İzmir Institute of Technology

Prof. Dr. Engin BÜYÜKAŞIK
Head of the Department of
Mathematics

Prof. Dr. Aysun SOFUOĞLU
Dean of the Graduate School of
Engineering and Sciences

ACKNOWLEDGMENTS

Foremost, I would like to express my sincere gratitude to my collaborator Assoc. Prof. Dr. Burak AKSOYLU for his encouragement in preparation of this thesis, his support, guidance and time spent in discussions throughout my studies. I would like to also thank my advisor Prof. Dr. Gamze TANOĞLU for her support in my difficult times. Of course, I would like to offer my special thanks to my wife Meryem KAYA, who has always been my source of strength and inspiration, for her encouragement, understanding and patience even during hard times of this study and to my son Abdullah Eren KAYA. Finally, I thank my family for creating physical and mental conditions for my education during my whole life.

ABSTRACT

NUMERICAL METHODS FOR NONLOCAL PROBLEMS

In this thesis, numerical methods for nonlocal problems with local boundary conditions from the area of peridynamics are studied. The novel operators that satisfy local boundary conditions were proposed as an alternative to the original nonlocal problems which uses nonlocal boundaries. Peridynamic theory is reformulation of continuum mechanics by integral equations for which it has some advantages over traditional partial differential equations. In peridynamic theory, a point can interact with other points within a certain distance which is called horizon and indicated by the parameter δ. In this thesis, we are particularly interested in role of the parameter δ in numerical methods for the novel problems. More precisely, we aim to show its role in condition number, discretization error and convergence factor of multigrid method.

ÖZET

YEREL OLMAYAN PROBLEMLER İÇİN SAYISAL YÖNTEMLER

Bu tezde, peridinamik alanında geçen yerel sınır şartlarını sağlayan yerel olmayan problemler için sayısal yöntemler çalışılmıştır. Yerel sınır şartlarını sağlayan bu yeni operatörler, yerel olmayan sınır şartlarını kullanan orjinal yerel olmayan operatörlere bir alternatif olarak tasarlanmıştır. Peridinamik teori sürekli ortamlar mekaniğinin integral denklemleri ile yeniden formülüze edilmesidir ve bu sayede kısmi diferansiyel denklemlere göre bazı avantajları vardır. Peridinamik teoride, bir nokta belirli bir uzaklık içindeki noktalar ile etkileşim içerisindedir. Bu uzaklığa horizon (ufuk) denir ve δ ile gösterilir. Bu tezde, özellikle δ parametresinin yerel olmayan problemler için sayısal yöntemlerdeki rolleriyle ilgileneceğiz. Daha kesin bir ifadeyle, δ parametresinin kondisyon sayısındaki, ayrıklaştırma hatasındaki ve multigrid metodunun yakınsaklık faktöründeki rollerini göstereceğiz.

TABLE OF CONTENTS

LIST OF FIGURES

Figure **Page**

LIST OF TABLES

CHAPTER 1

INTRODUCTION

Traditional partial differential equations (PDEs) consist of combinations of the unknown function and different orders of its derivatives. It is sufficient to know only values of the function in an arbitrarily small neighborhood of a point to check whether a PDE holds at that point. This information is not sufficient for a nonlocal equation to check whether it satisfies at that point because information about the values of the function far from that point is needed. Most of the time, this is because the equation involves integral operators Web (2014). Nonlocal equations are used, for instance, in peridynamics (PD) Silling (2000), nonlocal diffusion Andreu-Vaillo et al. (2010); Du et al. (2012), image processing Gilboa and Osher (2009), population models, particle systems, phase transition, and coagulation Du et al. (2012); Du and Lipton (2014); Silling and Lehoucq (2010); Madenci and Oterkus (2014).

PD theory aims to remodel the equations of continuum mechanics by replacing the PDEs of the classical theory with integral or integro-differential equations. The classical theory of solid mechanics assumes continuous distribution of mass within a body. It relies on PDEs and assumes sufficient smoothness of the deformation for the PDEs. The PDEs of the classical theory do not apply directly on a crack or dislocation because the deformation is discontinuous on these features. These considerations motivated the development of the PD theory which attempts to treat the evolution of discontinuities to the same field of equations as for continuous deformation. PD theory aims to relax the assumptions of classical theory of solid mechanics such as continuity, modeling of discrete particles and allowing the explicit modeling of nonlocal forces Silling and Lehoucq (2010). In literature, PD has been studied from different perspectives. The works Aksoylu and Mengesha (2010); Aksoylu and Parks (2011); Alali and Lipton (2012); Emmrich and Weckner (2007a,b); Mengesha and Du (2014b,a); Zhou and Du (2010) address the well-posedness for various forms, the works Aksoylu and Mengesha (2010); Aksoylu and Parks (2011); Aksoylu and Unlu (2014) address conditioning and variational theory and Aksoy and Senocak (2011); Aksoylu and Unlu (2014); Emmrich and Weckner (2007c); Tian and Du (2013); Seleson et al. (2013); Du et al. (2013) address the discretization and

numerical methods.

In nonlocal equations, a point can interact with other points within a certain distance which is called horizon and indicated by δ (see Figure 1.1). It is embedded in the support of the micromodulus function. The works by Aksoylu and Parks (2011); Aksoylu and Unlu (2014); Alali and Lipton (2012); Du and Zhou (2011); Emmrich and Weckner (2007b); Mengesha and Du (2014b,a); Silling and Lehoucq (2008); Zhou and Du (2010) aim to show connections between the nonlocal operator and the classical differential operator in the limit case $\delta \to 0$. Due to this interaction, nonlocal boundaries are used in nonlocal equations. We show the nonlocal boundaries $\mathcal{B}\Omega$ and bulk of the domain in 1D for $\Omega = [-1, 1]$ in Figure 1.2. Nonlocal boundary conditions cause problems in the

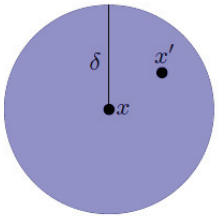

Figure 1.1. Horizon of the point x in 2D.

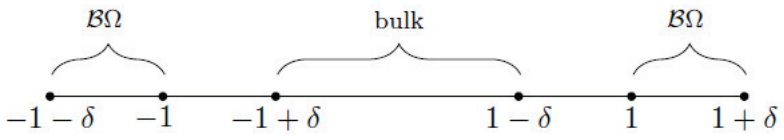

Figure 1.2. Nonlocal boundaries $\mathcal{B}\Omega$ and bulk of the domain in 1D for $\Omega = [-1, 1]$.

numerical solution of the nonlocal equations, which is called boundary effects. In order to mitigate boundary effects a lot of efforts are needed. For more informations related boundary effects, please refer to Madenci and Oterkus (2014); Kilic (2008). In order to

avoid nonlocal interactions at the boundaries and to handle problems that require local boundary conditions, authors in Beyer et al. (2016); Aksoylu et al. (2017a,b); Aksoylu and Celiker (2016, 2017); Aksoylu et al. (2018) recently discovered a way to incorporate local BC into nonlocal theories, in particular, into PD. In the unbounded domain case, authors discovered that the governing nonlocal operator is a function of a multiple of the classical governing operator Beyer et al. (2016). This opened a gateway to incorporate local boundary conditions into nonlocal theories Aksoylu et al. (2017b). These novel operators agree with the original PD operators proposed by Silling (2000) in the bulk of the domain in 1D. In other words, local boundary conditions are enforced by doing modifications to the original PD operator outside of the bulk of the domain.

In this thesis, numerical methods for nonlocal problems that satisfy local boundary conditions; periodic, antiperiodic, Dirichlet and Neumann, proposed in Aksoylu et al. (2017a); Aksoylu and Celiker (2017) are studied. We are particularly interested in the role of nonlocal parameter δ in numerical methods, such as condition number, discretization error and convergence rates of multigrid method. The rest of this thesis is structured as follows. In Chapter 2, we introduce novel nonlocal operators that satisfy local boundary conditions; periodic, antiperiodic, Dirichlet and Neumann, respectively and show how they satisfy these boundary conditions. In Chapter 3, we perform conditioning analysis. To accomplish this, we resort to the original continuous operators and present explicit expression of their eigenvalues in terms of δ. With the aid of some techniques from calculus, we find sharp bounds for the condition numbers for each problem and compare them with condition number of the corresponding system matrices. Corresponding system matrices are obtained by Nyström method with trapezoidal rule. We compare our results with the results in literature obtained for original PD operator. We also carry out error analysis under regularity assumptions and justify our result with numerical tests. Chapter 4 is devoted to convergence analysis of a multigrid method. To do this, we find eigenvalues of the resulting system matrices in terms of mesh size h and δ. We carry out a detailed smoother analysis. By finding the eigenvalues of the iteration matrix of the two-grid explicitly, we obtain a strict upper bound for the convergence factor. We numerically verify the upper bound. In Chapter 5, we summarize our results.

CHAPTER 2

NONLOCAL PROBLEMS WITH LOCAL BOUNDARIES

The original operator used in PD theory is given by

$$cu(x) - \int_{\Omega} C(x - x')u(x')dx' = f(x), \qquad x \in \Omega \tag{2.1}$$

where $C, u \in L^2(\Omega)$, $c = \int_{\Omega} C(x')dx'$. In this formulation, nonlocal boundaries are used. Nonlocal boundaries cause surface effects in numerical solutions and some problems in nature require local boundary conditions. So, it is important to develop nonlocal operators that use local boundary conditions that share almost the same characteristics with the original PD operator in (2.1). For this purpose, a series of papers Beyer et al. (2016); Aksoylu et al. (2017a,b); Aksoylu and Celiker (2016, 2017); Aksoylu et al. (2018) was published. In the unbounded domain case, authors discovered that the governing nonlocal operator is a function of multiple of the classical governing operator Beyer et al. (2016). This opened a gateway to incorporate local boundary conditions into nonlocal theories Aksoylu et al. (2017b). These novel operators agree with the original PD operator in the bulk of the domain in 1D. Furthermore, in the following chapter, we will show that their condition numbers have the same characteristic. Now, we introduce these novel operators in 1D, respectively. We choose $\Omega = [-1, 1]$ throughout the thesis just for simplicity. We show its extension to $[-2, 2]$ by $\widehat{\Omega}$.

2.1. Periodic Problem

We consider the following nonlocal equation

$$\mathcal{M}_{\mathrm{p}}u(x) = cu(x) - \mathcal{C}_{\mathrm{p}}u(x) = f(x) \tag{2.2}$$

which is convolution Fredholm second kind, where

$$\mathcal{C}_{\mathtt{p}}u(x) = \int_{\Omega} \widehat{C}_{\mathtt{p}}(x - x')u(x')dx'$$

and

$$c = \int_{\Omega} C(x')dx'.$$

In above equation, $\widehat{C}_{\mathtt{p}}$ is the periodic extension of the function $C(x)$. The function $C(x)$ we will consider throughout the thesis for all kinds of boundary conditions is in the following form

$$C(x) = \begin{cases} 1, & \text{if} \quad -\delta < x < \delta, \\ \\ 0, & \text{otherwise} \end{cases} \tag{2.3}$$

on $[-1, 1]$, where $0 < \delta < 1$. δ is the horizon of the problem. It is specific to the problem. $\widehat{C}_{\mathtt{p}}$ is represented in Figure 2.1. This choice of $C(x)$ aligns with the construction given in Aksoylu et al. (2017a), that is, $C(x) \in L^2(\Omega)$, and hence,

$$\widehat{C}_{\mathtt{p}}(x) \in L^2(\widehat{\Omega}).$$

Furthermore, we assume that

$$u(x), f(x) \in L^2(\Omega) \cap C^1(\partial\Omega).$$

Equation (2.2) is obtained from the following equation

$$cu(x) - \mathcal{C} *_{\mathtt{p}} u(x) = f(x),$$

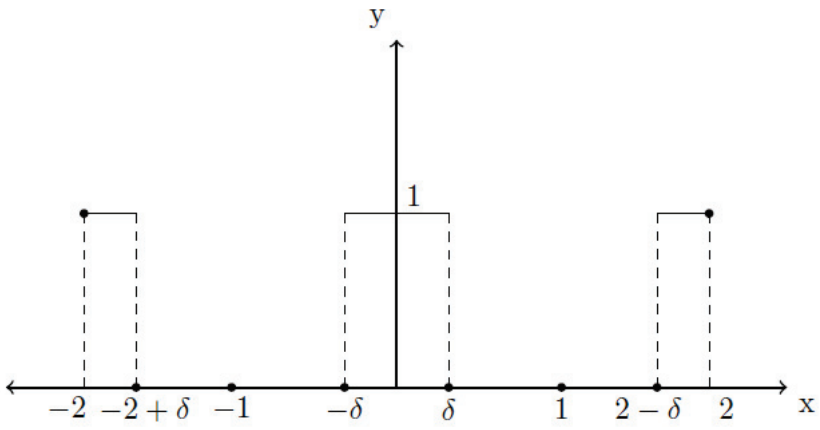

Figure 2.1. Periodic extension of $C(x)$ on $[-2, 2]$.

where

$$\mathcal{C} *_{\mathtt{p}} u := \sum_k \langle e_k^{\mathtt{p}} | C \rangle \, \langle e_k^{\mathtt{p}} | u \rangle \, e_k^{\mathtt{p}}.$$

Here, $\langle \cdot | \cdot \rangle$ denotes the inner product in $L^2(\Omega)$ and is defined by

$$\langle e_k^{\mathtt{p}} | u \rangle := \int_\Omega e_k^{\mathtt{p}}(x') u(x') dx'.$$

The functions $e_k^{\mathtt{p}}$ are eigenfunctions of $\mathcal{C}_{\mathtt{p}}$ and defined as $e_k^{\mathtt{p}} = e^{ik\pi x}$, $k \in \mathbb{N}$. We call $\mathcal{C}*_{\mathtt{p}}$ as abstract convolution. For more details, we refer to Aksoylu et al. (2017a).

We know from Aksoylu et al. (2017a) that the operator $\mathcal{C}_{\mathtt{p}}$ is Hilbert-Schmidt and hence it is self-adjoint and compact. $f(x)$ is a specified function satisfying periodic boundary conditions (compatibility condition) and $\int_\Omega f(x)dx = 0$ (Fredholm condition). With the above conditions on $f(x)$, Equation (2.2) satisfies Fredholm alternative that is it is solvable. However, since spectrum of $\mathcal{M}_{\mathtt{p}}$ has 0 eigenvalue, it has infinitely many solutions. To get a unique solution, one has to put a restriction on the solution u.

With simple algebraic manipulations, it is possible to write $\mathcal{C}_{\mathtt{p}} u(x)$ as follows:

$$\mathcal{C}_{\mathtt{p}}u(x) := -\begin{cases} \int_{-1}^{x+\delta} u(x')dx' + \int_{2+x-\delta}^{1} u(x')dx', & x \in [-1, -1+\delta), \\ \int_{x-\delta}^{x+\delta} u(x')dx', & x \in [-1+\delta, 1-\delta], \\ \int_{-1}^{x-2+\delta} u(x')dx' + \int_{x-\delta}^{1} u(x')dx', & x \in (1-\delta, 1]. \end{cases} \tag{2.4}$$

Solution of Equation (2.2) satisfies periodic boundary conditions. In order to verify this, we substitute the boundary points into Equation (2.2) and get

$$cu(-1) - \int_{-1}^{-1+\delta} u(x')dx' - \int_{1-\delta}^{1} u(x')dx' = f(-1) \tag{2.5}$$

and

$$cu(1) - \int_{-1}^{-1+\delta} u(x')dx' - \int_{1-\delta}^{1} u(x')dx' = f(1). \tag{2.6}$$

Subtracting Equation (2.6) from Equation (2.5), we get

$$c\,(u(-1) - u(1)) = f(-1) - f(1).$$

From the assumption on $f(x)$, $f(-1) = f(1)$. So, we arrive at $u(-1) = u(1)$. Taking the derivative of Equation (2.2), using the definition of $\mathcal{C}_{\mathtt{p}}$ in (2.4) and employing Fundamental Theorem of Calculus, we can show that $u'(-1) = u'(1)$.

2.2. Antiperiodic Problem

The antiperiodic problem we consider is the following convolution Fredholm second kind

$$\mathcal{M}_{\mathtt{a}}u(x) = cu(x) - \mathcal{C}_{\mathtt{a}}u(x) = f(x), \tag{2.7}$$

where

$$\mathcal{C}_{\mathtt{a}}u(x) = \int_{\Omega} \widehat{C}_a(x-x')u(x')dx' = f(x) \tag{2.8}$$

and

$$c = \int_{\Omega} C(x')dx'.$$

Here, $\widehat{C}_{\mathtt{a}}$ is the antiperiodic extension of the function $C(x)$ in (2.3) (see Figure 2.2). As in the case of the periodic problem,

$$\widehat{C}_{\mathtt{a}}(x) \in L^2(\widehat{\Omega})$$

and we assume that

$$u(x), f(x) \in L^2(\Omega) \cap C^1(\partial\Omega).$$

Equation (2.7) is obtained from the following abstract convolution

$$cu(x) - \mathcal{C} *_{\mathtt{a}} u(x) = f(x),$$

where

$$\mathcal{C} *_{\mathtt{a}} u := \sum_k \langle e_k^{\mathtt{a}}|C\rangle \, \langle e_k^{\mathtt{a}}|u\rangle \, e_k^{\mathtt{a}}.$$

The eigenfunctions of $\mathcal{C}_{\mathtt{a}}$ are defined by $e_k^{\mathtt{a}} = e^{i(k+\frac{1}{2})\pi x}$, $k \in \mathbb{N}$. Please, see Aksoylu et al. (2017a) for the details.

We know from Aksoylu et al. (2017a) that operator $\mathcal{C}_{\mathtt{a}}$ is Hilbrt-Schmidt and hence

it is self-adjoint and compact. $f(x)$ is a specified function satisfying antiperiodic boundary conditions (compatibility condition). We will show in Chapter 3 that the antiperiodic operator $\mathcal{M}_{\mathtt{a}}$ is positive definite. It satisfies Fredholm alternative that is, it has unique solution. It is same with the original PD operator in (2.1) in the bulk of the domain.

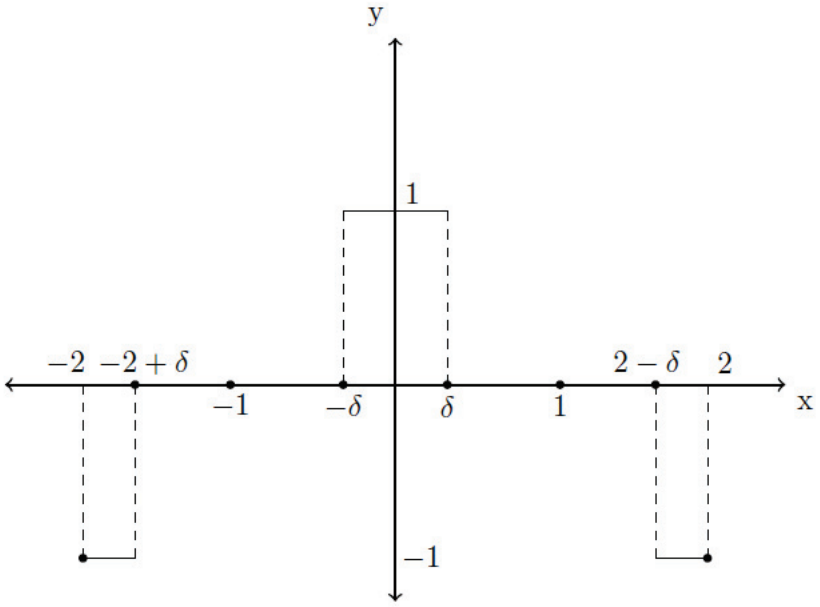

Figure 2.2. Antiperiodic extension of $C(x)$ on $[-2, 2]$.

One can write $\mathcal{C}_{\mathtt{a}}u(x)$ as follows:

$$\mathcal{C}_{\mathtt{a}}u(x) := -\begin{cases} \int_{-1}^{x+\delta} u(x')dx' - \int_{2+x-\delta}^{1} u(x')dx', & x \in [-1, -1+\delta), \\ \int_{x-\delta}^{x+\delta} u(x')dx', & x \in [-1+\delta, 1-\delta], \\ -\int_{-1}^{x-2+\delta} u(x')dx' + \int_{x-\delta}^{1} u(x')dx', & x \in (1-\delta, 1]. \end{cases} \tag{2.9}$$

Solution of Equation (2.7) satisfies antiperiodic boundary conditions. To see this, we substitute the boundary points into Equation (2.7) and get

$$cu(-1) - \int_{-1}^{-1+\delta} u(x')dx' + \int_{1}^{1-\delta} u(x')dx' = f(-1) \tag{2.10}$$

and

$$cu(1) + \int_{-1}^{-1+\delta} u(x')dx' - \int_{1}^{1-\delta} u(x')dx' = f(1). \tag{2.11}$$

Adding equations in (2.10) and (2.11), we get

$$c\left(u(-1) + u(1)\right) = f(-1) + f(1).$$

From the compatibility condition, $f(-1) = -f(1)$. Hence, we end up with $u(-1) = -u(1)$. Taking the derivative of Equation (2.7) and using the Fundamental Theorem of Calculus, we can show that $u'(-1) = -u'(1)$.

2.3. Neumann Problem

The Neumann problem we consider was proposed in Aksoylu and Celiker (2017) and is of the form

$$\mathcal{M}_{\mathtt{N}}u(x) = cu(x) - \mathcal{C}_{\mathtt{N}}u(x) = f(x), \tag{2.12}$$

where

$$\mathcal{C}_{\mathtt{N}}u(x) = \int_{\Omega} \left(\widehat{C}_{\mathtt{p}}(x-x')P_e + \widehat{C}_{\mathtt{a}}(x-x')P_o\right) u(x')dx'.$$

Here, c, $\widehat{C}_{\mathtt{p}}$, $\widehat{C}_{\mathtt{a}}$ are defined as before. P_e and P_o are the even and odd projections, respectively and they are defined by

$$P_e u(x') = \frac{u(x') + u(-x')}{2}, \qquad P_o u(x') = \frac{u(x') - u(-x')}{2}.$$

Equation (2.12) is equivalent to

$$cu(x) - (\mathcal{C} *_{\mathtt{p}} P_e + \mathcal{C} *_{\mathtt{a}} P_o)\, u(x) = f(x).$$

Since the operator $\mathcal{C}_{\mathtt{N}}$ is a linear combination of $\mathcal{C}_{\mathtt{p}}$ and $\mathcal{C}_{\mathtt{a}}$, it is also self-adjoint and compact. From Chapter 3, $\mathcal{M}_{\mathtt{N}}$ has zero eigenvalue with the corresponding eigenfunction 1. From the Fredholm alternative, Equation (2.12) is solvable on condition that $\int_\Omega f(x)dx = 0$ (Fredholm condition). Under this condition it has infinitely many solutions. To get a unique solution one has to put a restriction on the solution u. The Neumann operator $\mathcal{M}_{\mathtt{N}}$ is same with the original PD operator in (2.1) in the bulk of the domain. We will show in Chapter 3 that it is positive semidefinite. Again, we assume that

$$u(x), f(x) \in L^2(\Omega) \cap C^1(\partial\Omega).$$

$\mathcal{C}_{\mathtt{N}}u(x)$ can be written as

$$\mathcal{C}_{\mathtt{N}}u(x) := -\begin{cases} \int_{-1}^{x+\delta} u(x')dx' + \int_{-1}^{-2-x+\delta} u(x')dx', & x \in [-1, -1+\delta), \\ \int_{x-\delta}^{x+\delta} u(x')dx', & x \in [-1+\delta, 1-\delta], \\ \int_{x-\delta}^{1} u(x')dx' + \int_{-x+2-\delta}^{1} u(x')dx', & x \in (1-\delta, 1]. \end{cases} \tag{2.13}$$

At the boundaries, solution of Equation (2.12) satisfies $u'(-1) = f'(-1)/c$ and $u'(1) = f'(1)/c$. To verify these, first, we differentiate both sides of Equation (2.12) at $x = -1$. Using the definition of $\mathcal{C}_{\mathtt{N}}$ in (2.13) and Fundamental Theorem of Calculus, we obtain

$$cu'(x) - u(x+\delta) + u(-2-x+\delta) = f'(x).$$

Substituting -1 into the above equation we get

$$cu'(-1) = f'(-1).$$

Now, differentiating both sides of Equation (2.12) at $x = 1$ and using Fundamental Theorem of Calculus, we get

$$cu'(x) - u(x - \delta) + u(-x + 2 - \delta) = f'(x).$$

Substituting 1 into the above equation, we arrive at

$$cu'(1) = f'(1).$$

2.4. Dirichlet Problem

For Dirichlet problem, we consider

$$\mathcal{M}_{\mathtt{D}}u(x) = cu(x) - \mathcal{C}_{\mathtt{D}}u(x) = f(x), \tag{2.14}$$

where

$$\mathcal{C}_{\mathtt{D}}u(x) := \int_{\Omega} \left(\widehat{C}_{\mathtt{p}}(x - x')P_o + \widehat{C}_{\mathtt{a}}(x - x')P_e \right) u(x')dx'. \tag{2.15}$$

It was proposed in Aksoylu and Celiker (2017). In the above equation, c, $\widehat{C}_{\mathtt{p}}$, $\widehat{C}_{\mathtt{a}}$, P_e and P_o are defined as before. Equation (2.14) is equivalent to the following equation

$$cu(x) - \mathcal{C} *_{\mathtt{a}} P_e u(x) - \mathcal{C} *_{\mathtt{p}} P_o u(x) = f(x).$$

Since the operator $\mathcal{C}_{\mathtt{D}}$ is a linear combination of $\mathcal{C}_{\mathtt{p}}$ and $\mathcal{C}_{\mathtt{a}}$, it is also self-adjoint and compact. By the Fredholm alternative, Equation (2.14) has unique solution. The Dirichlet operator $\mathcal{M}_{\mathtt{D}}$ is same with the original PD operator in (2.1) in the bulk of the domain. We

will show in Chapter 3 that it is positive definite. In this case, we assume that

$$u(x), f(x) \in L^2(\Omega).$$

It is possible to write $\mathcal{C}_{\mathtt{D}}u(x)$ as

$$\mathcal{C}_{\mathtt{D}}u(x) := -\begin{cases} \int_{-1}^{x+\delta} u(x')dx' - \int_{-1}^{-2-x+\delta} u(x')dx', & x \in [-1, -1+\delta), \\ \int_{x-\delta}^{x+\delta} u(x')dx', & x \in [-1+\delta, 1-\delta], \\ \int_{x-\delta}^{1} u(x')dx' - \int_{-x+2-\delta}^{1} u(x')dx', & x \in (1-\delta, 1]. \end{cases} \tag{2.16}$$

Substituting boundary nodes into Equation (2.14) and using the definition of $\mathcal{C}_{\mathtt{D}}$ in (2.16), one can easily verify that Equation (2.14) satisfies $u(-1) = f(-1)/c$ and $u(1) = f(1)/c$ at $x = -1$ and $x = 1$, respectively.

CHAPTER 3

CONDITIONING AND ERROR ANALYSES

In this chapter, we carry out conditioning and error analyses for the novel operators. We find sharp bounds for the condition numbers of the original continuous operators in terms of δ and numerically compare them with the condition numbers of the corresponding discrete problems. Under regularity assumption, we carry out error analysis for Nyström method with trapezoidal rule. Results of Chapter 3 has already been published in Aksoylu and Kaya (2018a).

3.1. The Periodic and Antiperiodic Operators and Their Eigenvalues

In Aksoylu and Celiker (2017), for $u, C \in L^2(\Omega)$, it is proved that the operators $\mathcal{C}_{\mathtt{BC}}$, $\mathtt{BC} = \{\mathtt{p}, \mathtt{a}\}$ has the following integral representations

$$\mathcal{C}_{\mathtt{p}}u(x) = \int_{\Omega} \widehat{C}_{\mathtt{p}}(x' - x)u(x')dx', \quad \mathcal{C}_{\mathtt{a}}u(x) = \int_{\Omega} \widehat{C}_{\mathtt{a}}(x' - x)u(x')dx'. \tag{3.1}$$

However, for our purposes, we turn to the series representation to obtain the eigenvalues of the operators $\mathcal{M}_{\mathtt{p}}$ and $\mathcal{M}_{\mathtt{a}}$. First, note that both operators $\Delta_{\mathtt{p}}$ and $\Delta_{\mathtt{a}}$ have a purely discrete spectrum consisting of the following eigenvalues

$$\sigma(\Delta_{\mathtt{p}}) = \left\{k^2 : k \in \mathbb{N}\right\}, \quad \sigma(\Delta_{\mathtt{a}}) = \left\{(k + \frac{1}{2})^2 : k \in \mathbb{N}\right\}$$

with the corresponding eigenfunctions

$$e_k^{\mathtt{p}}(x) := e^{i\pi kx}, \quad e_k^{\mathtt{a}}(x) := e^{i\pi(k+\frac{1}{2})x}, \quad k \in \mathbb{N}.$$

Furthermore, the operators $\mathcal{M}_{\mathtt{p}}$ and $\mathcal{M}_{\mathtt{a}}$ are self-adjoint. Hence, the condition number calculation reduces to finding

$$\kappa_e(\mathcal{M}_{\mathtt{p}}) = \frac{\lambda^{\mathtt{p}}_{\max}}{\lambda^{\mathtt{p}}_{\min,2}} \quad \text{and} \quad \kappa(\mathcal{M}_{\mathtt{a}}) = \frac{\lambda^{\mathtt{a}}_{\max}}{\lambda^{\mathtt{a}}_{\min}}. \tag{3.2}$$

Throughout the paper, we use the canonical kernel in (2.3), i.e., $C(x) = \chi_\delta(x)$. One can easily find the eigenvalues of the operators $\mathcal{M}_{\mathtt{p}}$ and $\mathcal{M}_{\mathtt{a}}$, given, respectively, as follows:

$$\lambda^{\mathtt{p}}_k = 2\delta - \langle e^{\mathtt{p}}_k | C\rangle = \begin{cases} 2\delta - \dfrac{2\sin(k\pi\delta)}{k\pi}, & k \in \mathbb{N}^* \\ 0, & k = 0, \end{cases} \tag{3.3}$$

$$\lambda^{\mathtt{a}}_k = 2\delta - \langle e^{\mathtt{a}}_k | C\rangle = 2\delta - \frac{2\sin((k+\frac{1}{2})\pi\delta)}{(k+\frac{1}{2})\pi}, \quad k \in \mathbb{N}. \tag{3.4}$$

Using continuous extension, we utilize the well-known cardinal sine function defined by

$$\operatorname{sinc}(\theta) := \frac{\sin(\theta)}{\theta}, \quad \theta \geq 0.$$

See Figure 3.1. The following function is utilized in the expression of eigenvalues of the operators $\mathcal{M}_{\mathtt{p}}$ and $\mathcal{M}_{\mathtt{a}}$.

$$\lambda(\theta) = 2\delta\big(1 - \operatorname{sinc}(\theta)\big) \tag{3.5}$$

Notice that the expressions of $\lambda^{\mathtt{p}}_k$ and $\lambda^{\mathtt{a}}_k$ both contain the same function in (3.5), but evaluated at different points:

$$\lambda^{\mathtt{p}}_k = \lambda(\theta^{\mathtt{p}}_k), \quad \lambda^{\mathtt{a}}_k = \lambda(\theta^{\mathtt{a}}_k),$$

where $\theta^{\mathtt{p}}_k = k\pi\delta,\ k \in \mathbb{N}$ and $\theta^{\mathtt{a}}_k = \frac{1}{2}(\pi\delta + 2k\pi\delta),\ k \in \mathbb{N}$. We immediately see that

$$0 \leq \lambda^{\mathtt{p}}_k, \quad 0 < \lambda^{\mathtt{a}}_k.$$

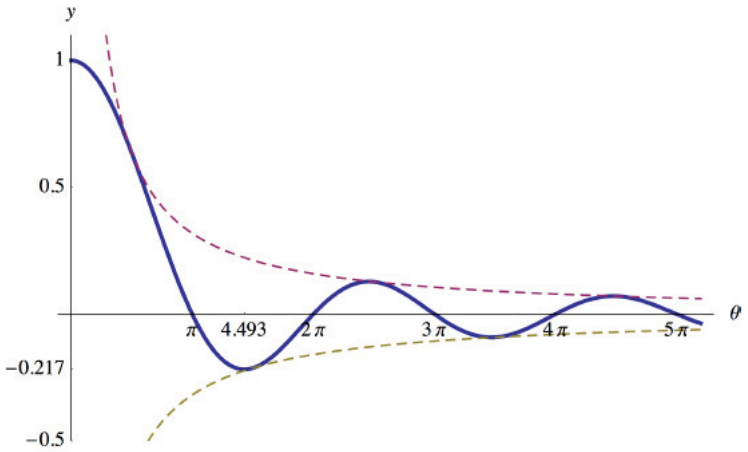

Figure 3.1. Graph of $\text{sinc}(\theta) = \dfrac{\sin(\theta)}{\theta}$ (solid line) and $\dfrac{\pm 1}{\theta}$ (dashed lines).

Furthermore, using basic calculus, for $\theta > 0$, it is easy to prove that

$$0 < 1 - \text{sinc}(\theta) < \frac{3}{2}. \tag{3.6}$$

Hence, it is more suitable to work with the expression in (3.5).

3.2. Sharp Bounds for the Condition Number

3.2.1. The Periodic Operator

It is easy to see that $\lambda_{\min}^{\mathsf{p}}$ occurs when $\text{sinc}(\theta)$ is at its maximum, which occurs when $k = 0$. This leads to $\lambda_{\min}^{\mathsf{p}} = 0$. It means that for the condition number estimate, we have to utilize the effective condition number, which requires the next positive minimum eigenvalue $\lambda_{\min,2}$. We prepare for finding the exact expression of $\lambda_{\min,2}$.

Lemma 3.2.1 *For $\delta \in (0, 1)$, the following inequality holds.*

$$\frac{\sin(k\pi\delta)}{k\pi} < \frac{\sin(\pi\delta)}{\pi}, \quad k = 2, 3, \dots . \tag{3.7}$$

Proof The inequality (3.7) is equivalent to

$$\sin(k\delta\pi) < k\sin(\pi\delta), \quad k = 2, 3, \dots .$$

We have two cases: If $\sin(k\pi\delta) \leq \sin(\pi\delta)$, then the proof is straightforward. Now, we consider the case

$$\sin(\pi\delta) < \sin(k\pi\delta). \tag{3.8}$$

We proceed by induction.

• **Induction step 1:** For $k = 2$, we want to prove that

$$\sin(2\pi\delta) < 2\sin(\pi\delta).$$

To do so, we define the function

$$f(\delta) := 2\sin(\pi\delta) - \sin(2\pi\delta),$$

and aim to show that $f(\delta) > 0$. We start by finding the extremal values of f. Note that $f(\delta)$ has only one critical point in the interval $(0, 1)$, i.e., $\delta = \frac{2}{3}$, for which we have $f(\frac{2}{3}) = \frac{3\sqrt{3}}{2}$. After some simple calculation, we obtain that f is monotone increasing and decreasing on $(0, \frac{2}{3})$ and $(\frac{2}{3}, 1)$, respectively. Using the fact $f(0) = f(1) = 0$ and combining the monotonicity information, we obtain $0 < f(\delta) \leq \frac{3\sqrt{3}}{2}, \delta \in (0, 1)$, which leads to the desired result.

• **Induction step 2:** We start with the following induction assumption for arbitrary $k > 2$.

$$\sin(k\pi\delta) < k\sin(\pi\delta). \tag{3.9}$$

We aim to show that (3.9) holds for $k+1$. Using $0 < \sin(\pi\delta)$ and (3.8), we obtain

$$0 < \sin(k\pi\delta). \tag{3.10}$$

Using $\cos(\pi\delta) < 1$ and (3.10), we obtain

$$\cos(\pi\delta)\sin(k\pi\delta) < \sin(k\pi\delta). \tag{3.11}$$

Using (3.11) and the induction assumption (3.9), we arrive at

$$\cos(\pi\delta)\sin(k\pi\delta) < k\sin(\pi\delta). \tag{3.12}$$

Using $\cos(k\pi\delta) \leq 1$, we have

$$\sin(\pi\delta)\cos(k\pi\delta) \leq \sin(\pi\delta). \tag{3.13}$$

Combining (3.12) and (3.13), we arrive at

$$\sin((k+1)\pi\delta) < (k+1)\sin(\pi\delta).$$

□

From (3.3), the positive minimum eigenvalue occurs when $k \geq 1$ and by Lemma 3.2.1, it occurs when $k = 1$. More precisely,

$$\lambda^{\mathtt{p}}_{\min,2} = 2\delta - \frac{2\sin(\pi\delta)}{\pi}. \tag{3.14}$$

On the other hand, the maximum eigenvalue occurs when $\sin(k\pi\delta) < 0$ for some $k \geq 2$. Using (3.6), we immediately conclude that

$$2\delta < \lambda^{\mathtt{p}}_{\max} < 3\delta. \tag{3.15}$$

In fact, it is possible to find an approximate upper bound smaller than the one given in (3.15). Let's define

$$\text{sinc}_{\min} := \min_{\theta \geq 0} \text{sinc}(\theta).$$

One can compute that $\text{sinc}_{\min} \approx \text{sinc}(4.493) \approx -0.217$; see Figure 3.1. Hence, the improved upper bound in (3.15) is approximately $2.434\,\delta$. For rigorous treatment, we work with the analytic upper bound in (3.15).

Rather than working with $\lambda^{\mathtt{p}}_{\min,2}$ and $\lambda^{\mathtt{p}}_{\max}$, we find it more convenient working directly with the effective condition number $\kappa_e(\mathcal{M}_{\mathtt{p}})$ given in (3.2) whose bounds are obtained by combining (3.14) and (3.15) as follows:

$$\frac{2\delta}{2\delta - \dfrac{2\sin(\pi\delta)}{\pi}} < \kappa_e(\mathcal{M}_{\mathtt{p}}) < \frac{3\delta}{2\delta - \dfrac{2\sin(\pi\delta)}{\pi}}. \tag{3.16}$$

We find bounds which have simpler form than the ones given in (3.16).

Lemma 3.2.2 *For $\delta \in (0,1)$, the following bounds hold.*

(Periodic-Lower Bound) $$\frac{6}{\pi^2}\delta^{-2} < \frac{2\delta}{2\delta - \dfrac{2\sin(\pi\delta)}{\pi}}, \tag{3.17}$$

(Periodic-Upper Bound) $$\frac{3\delta}{2\delta - \dfrac{2\sin(\pi\delta)}{\pi}} < \frac{24}{\pi^2}\delta^{-2}. \tag{3.18}$$

Proof (Periodic-Lower Bound): The inequality (3.17) is equivalent to proving

$$\frac{6}{x^2} < \frac{1}{1 - \text{sinc}(x)},$$

for $x = \delta\pi$ with $0 < x < \pi$. Hence, we aim to show that

$$0 < f(x) = x^3 - 6x + 6\sin(x).$$

Since

$$\lim_{x\to 0} f(x) = 0,$$

proving that $f(x) > 0$ follows from showing that $f(x)$ is strictly increasing. Namely,

$$0 < f'(x) = 3x^2 - 6 + 6\cos(x).$$

Hence, we need to consider the second and third derivatives of $f(x)$ given as

$$f''(x) = 6x - 6\sin(x), \quad f^{(3)}(x) = 6(1 - \cos(x)).$$

We also have

$$\lim_{x\to 0} f'(x) = \lim_{x\to 0} f''(x) = \lim_{x\to 0} f^{(3)}(x) = 0.$$

It is clear that $f^{(3)}(x) > 0$. This implies that $f''(x)$ is strictly increasing and from the limit value of $f''(x)$ at $x = 0$, $f''(x) > 0$. Similarly, this implies $f'(x)$ is strictly increasing and from the limit value of $f'(x)$ at $x = 0$, $f'(x) > 0$.
(Periodic-Upper Bound): The inequality (3.18) is equivalent to proving

$$\frac{3/2}{1 - \text{sinc}(x)} < \frac{24}{x^2},$$

for $x = \delta\pi$ with $0 < x < \pi$. Hence, we aim to show that

$$0 < f(x) = -3x^3 + 48x - 48\sin(x).$$

Since

$$\lim_{x \to 0} f(x) = 0,$$

proving that $f(x) > 0$ follows from showing that $f(x)$ is strictly increasing. Namely,

$$0 < f'(x) = -9x^2 + 48 - 48\cos(x).$$

Hence, we need to consider the second derivative of $f(x)$ given as

$$f''(x) = -18x + 48\sin(x).$$

We also have

$$\lim_{x \to 0} f''(x) = 0.$$

By the roots of $f''(x)$, we immediately see that

$$\text{sinc}(x) = \frac{3}{8}. \tag{3.19}$$

The function $\text{sinc}(x)$ is one-to-one for $0 < x < \pi$ and $\frac{3}{8}$ is in the range of the function. Hence, Equation (3.19) has only one solution. So, $f''(x)$ has only one root and denote it by x^*. Since

$$\lim_{x \to \pi} f''(x) = -18\pi < 0,$$

it follows that $f''(x) > 0$ for $0 < x < x^*$ and $f''(x) < 0$ for $x^* < x < \pi$. Combining the above calculations, the function $f''(x)$ leads to the fact that $f'(x)$ has only one critical

point at $x = x^*$ and $f'(x)$ is increasing for $0 < x < x^*$ and decreasing for $x^* < x < \pi$. Since

$$\lim_{x\to 0} f'(x) = 0, \quad \lim_{x\to \pi} f'(x) = 96 - 9\pi^2 > 0,$$

finally, we arrive at $f'(x) > 0$ for $0 < x < \pi$.

□

Combining (3.17) and (3.18), finally, we arrive at the sharp condition number bounds

$$\frac{6}{\pi^2}\delta^{-2} < \kappa_e(\mathcal{M}_{\mathtt{p}}) < \frac{24}{\pi^2}\delta^{-2}. \tag{3.20}$$

for the periodic operator $\mathcal{M}_{\mathtt{p}}$.

3.2.2. The Antiperiodic Operator

Similar to $\lambda^{\mathtt{p}}_{\min}$, $\lambda^{\mathtt{a}}_{\min}$ occurs when $\mathrm{sinc}(\theta)$ is at its maximum, which occurs when $\theta = (k + \frac{1}{2})\pi\delta$ is closest to 0 for $k \in \mathbb{N}$. Then, we get $k = [\frac{-1}{2}] = 0$. Hence, using (3.4), we obtain

$$\lambda^{\mathtt{a}}_{\min} = 2\delta - \frac{2\sin(\pi/2\,\delta)}{\pi/2}. \tag{3.21}$$

On the other hand, since the eigenvalues $\lambda^{\mathtt{a}}_k$ sweep the values of the function for $\lambda^{\mathtt{p}}_k$ in (3.5), the same bounds in (3.6) are also valid for $\lambda^{\mathtt{a}}_k$. More precisely,

$$2\delta < \lambda^{\mathtt{a}}_{\max} < 3\delta. \tag{3.22}$$

Similar to (3.16), combining (3.21) and (3.22), we arrive at the following bounds

$$\frac{2\delta}{2\delta - \dfrac{2\sin(\pi/2\,\delta)}{\pi/2}} < \kappa(\mathcal{M}_{\mathtt{a}}) < \frac{3\delta}{2\delta - \dfrac{2\sin(\pi/2\,\delta)}{\pi/2}}. \tag{3.23}$$

We find bounds which have simpler form than the ones given in (3.23).

Lemma 3.2.3 *For $\delta \in (0,1)$, the following bounds hold.*

(Antiperiodic-Lower Bound)
$$\frac{24}{\pi^2}\delta^{-2} < \frac{2\delta}{2\delta - \dfrac{2\sin(\pi/2\,\delta)}{\pi/2}}, \tag{3.24}$$

(Antiperiodic-Upper Bound)
$$\frac{3\delta}{2\delta - \dfrac{2\sin(\pi/2\,\delta)}{\pi/2}} < \frac{96}{\pi^2}\delta^{-2}. \tag{3.25}$$

Proof (Antiperiodic-Lower Bound): The inequality (3.24) is equivalent to proving

$$\frac{6}{x^2} < \frac{1}{1-\operatorname{sinc}(x)},$$

for $x = \frac{\delta\pi}{2}$ with $0 < x < \frac{\pi}{2}$, which has already been proved in Lemma 3.2.2 for $0 < x < \pi$.

(Antiperiodic-Upper Bound): The inequality (3.25) is equivalent to proving

$$\frac{3/2}{1-\operatorname{sinc}(x)} < \frac{24}{x^2},$$

for $x = \frac{\delta\pi}{2}$ with $0 < x < \frac{\pi}{2}$, which has already been proved in Lemma 3.2.2 for $0 < x < \pi$.

□

Combining (3.24) and (3.25), finally, we arrive at the sharp condition number bounds

$$\frac{24}{\pi^2}\delta^{-2} < \kappa(\mathcal{M}_{\mathtt{a}}) < \frac{96}{\pi^2}\delta^{-2}. \tag{3.26}$$

for the antiperiodic operator $\mathcal{M}_{\mathtt{a}}$.

3.2.3. The Neumann and Dirichlet Operators

We can express the operators $\mathcal{M}_{\mathtt{N}}$ and $\mathcal{M}_{\mathtt{D}}$ using the operators $\mathcal{C}_{\mathtt{p}}$ and $\mathcal{C}_{\mathtt{a}}$ as follows:

$$\begin{aligned}\big(\mathcal{M}_{\mathtt{N}} - c\big)u(x) &= -\big(\mathcal{C}_{\mathtt{a}}P_o + \mathcal{C}_{\mathtt{p}}P_e\big)u(x),\\ \big(\mathcal{M}_{\mathtt{D}} - c\big)u(x) &= -\big(\mathcal{C}_{\mathtt{a}}P_e + \mathcal{C}_{\mathtt{p}}P_o\big)u(x).\end{aligned}$$

Note that the orthogonal projections P_e and P_o have the following properties

$$P_e^2 = P_e, \quad P_o^2 = P_o, \quad P_eP_o = P_oP_e = 0. \tag{3.27}$$

We present a commutativity property that will help us in finding $\sigma(\mathcal{M}_{\mathtt{N}})$ and $\sigma(\mathcal{M}_{\mathtt{D}})$.

Lemma 3.2.4

$$\mathcal{C}_{\mathtt{a}}P_e = P_e\mathcal{C}_{\mathtt{a}}, \quad \mathcal{C}_{\mathtt{a}}P_o = P_o\mathcal{C}_{\mathtt{a}}, \quad \mathcal{C}_{\mathtt{p}}P_e = P_e\mathcal{C}_{\mathtt{p}}, \quad \mathcal{C}_{\mathtt{p}}P_o = P_o\mathcal{C}_{\mathtt{p}}. \tag{3.28}$$

Proof We present the proof for $\mathcal{C}_{\mathtt{a}}P_e = P_e\mathcal{C}_{\mathtt{a}}$. The other results easily follow. We recall the definition of $\mathcal{C}_{\mathtt{a}}u(x)$ in (3.1). We explicitly write $P_e\mathcal{C}_{\mathtt{a}}u(x)$. The result follows by a change of variable.

$$\begin{aligned}P_e\mathcal{C}_{\mathtt{a}}u(x) &= \frac{1}{2}\Big(\int_\Omega \widehat{C}_{\mathtt{a}}(x'-x)u(x')dx' + \int_\Omega \widehat{C}_{\mathtt{a}}(x'+x)u(x')dx'\Big)\\ &= \frac{1}{2}\Big(\int_\Omega \widehat{C}_{\mathtt{a}}(x'-x)u(x')dx' + \int_\Omega \widehat{C}_{\mathtt{a}}(x'-x)u(-x')dx'\Big)\\ &= \int_\Omega \widehat{C}_{\mathtt{a}}(x'-x)P_eu(x')dx' \;=\; \mathcal{C}_{\mathtt{a}}P_eu(x)\end{aligned}$$

□

We are now in a position to present the main spectral results for the operators $\mathcal{M}_{\mathtt{N}}$ and $\mathcal{M}_{\mathtt{D}}$.

Lemma 3.2.5 *The spectra of the operators $\mathcal{M}_{\mathtt{N}}$ and $\mathcal{M}_{\mathtt{D}}$ are as follows:*

$$\sigma(\mathcal{M}_{\mathtt{N}}) = \sigma(\mathcal{M}_{\mathtt{a}}) \cup \sigma(\mathcal{M}_{\mathtt{p}}) \quad \textit{and} \quad \sigma(\mathcal{M}_{\mathtt{D}}) = \sigma(\mathcal{M}_{\mathtt{a}}) \cup \sigma(\mathcal{M}_{\mathtt{p}}) \setminus \{0\}. \tag{3.29}$$

Proof We present the result for $\mathcal{M}_{\mathtt{D}}$ only. The result for the case of $\mathcal{M}_{\mathtt{N}}$ follows in a similar way. It is obvious that $\sigma(\mathcal{M}_{\mathtt{D}}) = \sigma(\mathcal{M}_{\mathtt{D}} - c) + c$ and is more convenient to work with $\sigma(\mathcal{M}_{\mathtt{D}} - c)$.

- $\sigma(\mathcal{M}_{\mathtt{p}} - c) \cup \sigma(\mathcal{M}_{\mathtt{a}} - c) \subset \sigma(\mathcal{M}_{\mathtt{D}} - c)$:

Let $\lambda^{\mathtt{a}} \in \sigma(\mathcal{M}_{\mathtt{a}} - c)$. Namely, there exists an eigenfunction $u^{\mathtt{a}}$ satisfying $\big(\mathcal{M}_{\mathtt{a}} - c\big)u^{\mathtt{a}} = \lambda^{\mathtt{a}} u^{\mathtt{a}}$. Define $v^{\mathtt{a}} := P_e u^{\mathtt{a}}$. Then, using the properties $P_e^2 = P_e$ and $P_o P_e = 0$ given in (3.27), we obtain

$$\begin{aligned} \big(\mathcal{M}_{\mathtt{D}} - c\big)v^{\mathtt{a}} &= -\big(\mathcal{C}_{\mathtt{a}} P_e + \mathcal{C}_{\mathtt{p}} P_o\big) P_e u^{\mathtt{a}} = -\mathcal{C}_{\mathtt{a}} P_e u^{\mathtt{a}} \\ &= -P_e \mathcal{C}_{\mathtt{a}} u^{\mathtt{a}} = P_e\big(\mathcal{M}_{\mathtt{a}} - c\big)u^{\mathtt{a}} = \lambda^{\mathtt{a}} P_e u^{\mathtt{a}} = \lambda^{\mathtt{a}} v^{\mathtt{a}}. \end{aligned} \tag{3.30}$$

Hence, $\sigma(\mathcal{M}_{\mathtt{a}} - c) \subset \sigma(\mathcal{M}_{\mathtt{D}} - c)$.

Similarly, let $\lambda^{\mathtt{p}} \in \sigma(\mathcal{M}_{\mathtt{p}} - c)$. Namely, there exists an eigenfunction $u^{\mathtt{p}}$ $\big(\mathcal{M}_{\mathtt{p}} - c\big)u^{\mathtt{p}} = \lambda^{\mathtt{p}} u^{\mathtt{p}}$. Define $v^{\mathtt{p}} := P_o u^{\mathtt{p}}$. Note that $0 \in \sigma(\mathcal{M}_{\mathtt{p}} - c) = \sigma(\mathcal{C}_{\mathtt{p}})$ with the corresponding eigenfunction $u^{\mathtt{p}} = 1$. Since $v^{\mathtt{p}} = P_o 1 = 0$, we cannot utilize it as an eigenfunction, hence, the value 0 needs to be excluded. Then, using $P_o^2 = P_o$ and $P_e P_o = 0$, we obtain

$$\begin{aligned} \big(\mathcal{M}_{\mathtt{D}} - c\big)v^{\mathtt{p}} &= -\big(\mathcal{C}_{\mathtt{a}} P_e + \mathcal{C}_{\mathtt{p}} P_o\big) P_o u^{\mathtt{p}} = -\mathcal{C}_{\mathtt{p}} P_o u^{\mathtt{p}} \\ &= -P_o \mathcal{C}_{\mathtt{p}} u^{\mathtt{p}} = P_o\big(\mathcal{M}_{\mathtt{p}} - c\big)u^{\mathtt{p}} = \lambda^{\mathtt{p}} P_o u^{\mathtt{p}} = \lambda^{\mathtt{p}} v^{\mathtt{p}}. \end{aligned} \tag{3.31}$$

Hence, $\sigma(\mathcal{M}_{\mathtt{p}} - c) \subset \sigma(\mathcal{M}_{\mathtt{D}} - c)$. Combining (3.30) and (3.31), the result follows:

- $\sigma(\mathcal{M}_{\mathtt{D}} - c) \subset \sigma(\mathcal{M}_{\mathtt{p}} - c) \cup \sigma(\mathcal{M}_{\mathtt{a}} - c)$:

Let $\lambda^{\mathtt{D}} \in \sigma(\mathcal{M}_{\mathtt{D}} - c)$. Namely, $\big(\mathcal{M}_{\mathtt{D}} - c\big)u^{\mathtt{D}} = \lambda^{\mathtt{D}}u^{\mathtt{D}}$. Then, decompose $u^{\mathtt{D}}$ as follows:

$$-\big(\mathcal{C}_{\mathtt{a}}P_e + \mathcal{C}_{\mathtt{p}}P_o\big)(P_e + P_o)u^{\mathtt{D}} = \lambda^{\mathtt{D}}(P_e + P_o)u^{\mathtt{D}}.$$

Collecting the terms with P_e and P_o on each side and using commutativity in (3.28), we obtain

$$P_e\big(-\mathcal{C}_{\mathtt{a}} - \lambda^{\mathtt{D}}\big)u^{\mathtt{D}} + P_o\big(-\mathcal{C}_{\mathtt{p}} - \lambda^{\mathtt{D}}\big)u^{\mathtt{D}} = 0. \tag{3.32}$$

Since the operators P_e and P_o are orthogonal projections, each term in (3.32) must be equal to the zero function. Hence, we arrive at

$$\big(\mathcal{M}_{\mathtt{a}} - c\big)P_e u^{\mathtt{D}} = -\mathcal{C}_{\mathtt{a}}P_e u^{\mathtt{D}} = \lambda^{\mathtt{D}}P_e u^{\mathtt{D}},$$

$$\big(\mathcal{M}_{\mathtt{p}} - c\big)P_o u^{\mathtt{D}} = -\mathcal{C}_{\mathtt{p}}P_o u^{\mathtt{D}} = \lambda^{\mathtt{D}}P_o u^{\mathtt{D}}.$$

Consequently, $\lambda^{\mathtt{D}} \in \sigma(\mathcal{M}_{\mathtt{a}} - c) \cup \sigma(\mathcal{M}_{\mathtt{p}} - c)$.

□

The condition numbers of the operators $\mathcal{M}_{\mathtt{D}}$ and $\mathcal{M}_{\mathtt{N}}$ easily follow from the spectral result in (3.29).

Corollary 3.2.6

$$\kappa_e(\mathcal{M}_{\mathtt{N}}) = \kappa(\mathcal{M}_{\mathtt{D}}) = \frac{\max\{\lambda^{\mathtt{p}}_{\max}, \lambda^{\mathtt{a}}_{\max}\}}{\min\{\lambda^{\mathtt{p}}_{\min,2}, \lambda^{\mathtt{a}}_{\min}\}}.$$

Recalling the values of $\lambda^{\mathtt{p}}_{\min,2}$ in (3.14) and $\lambda^{\mathtt{a}}_{\min}$ in (3.21), we immediately see that

$$0 < \lambda^{\mathtt{a}}_{\min} \leq \lambda^{\mathtt{p}}_{\min,2}.$$

Hence, the condition numbers reduce to

$$\kappa_e(\mathcal{M}_{\mathtt{N}}) = \kappa(\mathcal{M}_{\mathtt{D}}) = \frac{\max\{\lambda^{\mathtt{p}}_{\max}, \lambda^{\mathtt{a}}_{\max}\}}{\lambda^{\mathtt{a}}_{\min}}. \tag{3.33}$$

On the other hand, we have the same bounds for $\lambda^{\mathtt{p}}_{\max}$ and $\lambda^{\mathtt{a}}_{\max}$ using (3.15) and (3.22), respectively. Consequently, combining this fact with (3.33), the bounds for the condition numbers $\kappa(\mathcal{M}_{\mathtt{D}})$ and $\kappa_e(\mathcal{M}_{\mathtt{N}})$ are identical to those of the antiperiodic operator $\mathcal{M}_{\mathtt{a}}$ given in (3.23). Hence, the bounds provided in Lemma 3.2.3 are valid for $\kappa_e(\mathcal{M}_{\mathtt{N}})$ and $\kappa(\mathcal{M}_{\mathtt{D}})$.

3.3. The Discretization and the Quadrature Rule

Our governing operators fall into the class of Fredholm integral equations of the second kind. The projection and the Nyström methods are the well-known types of discretization for this class (Atkinson, 1997, Chap. 3,4). We employ the Nyström method. We are dealing with integral equations, so, one has to pay special attention to the quadrature rule. Since the overarching goal of this study is to accommodate local BC, it is essential to use values at boundary nodes in the quadrature rule. The Gaussian quadrature rule is not suitable because it does not use boundary nodes. However, both the trapezoidal and the Simpson rules use boundary nodes, and hence, are plausible for such a task.

Furthermore, since the governing operator is self-adjoint, a discretization that produces symmetric matrices is desirable. Since the Simpson rule is more involved, obtaining symmetric matrices seems more cumbersome than that from the trapezoidal rule. The trapezoidal rule allows us to obtain symmetric matrices by simple algebraic manipulations; see Sec. 3.3.1. Consequently, we employ the trapezoidal rule. We choose the following uniformly distributed set of points x_i, $i = 1, ..., n$ in $[-1, 1]$. To discretize the equation

$$cu(x) - \mathcal{C}_{\mathtt{BC}}u(x) = f(x),$$

$\mathtt{BC} = \{\mathtt{p}, \mathtt{a}, \mathtt{N}, \mathtt{D}\}$, we let x run through points x_i. This yields

$$cu(x_i) - \mathcal{C}_{\mathtt{BC}} u(x_i) = f(x_i), \qquad i = 1, ..., n.$$

Then, apply trapezoidal rule setting the set of points x_i, $i = 1, ..., n$ as quadrature points to the integrals in (2.4,2.9,2.13,2.16). After the discretization, we get the following system of equation

$$A_{\mathtt{BC}} u_h = f_h,$$

$\mathtt{BC} = \{\mathtt{p}, \mathtt{a}, \mathtt{N}, \mathtt{D}\}$. Here, the system matrices $A_{\mathtt{BC}}$, $\mathtt{BC} = \{\mathtt{p}, \mathtt{a}, \mathtt{N}, \mathtt{D}\}$ are nonsymmetric. Note that, in our discretization, the ratio δ/h is always a positive integer and n is odd. In the rest of the thesis, d stands for δ/h.

3.3.1. Obtaining Symmetric System Matrices and Their Structures

The governing operator is self-adjoint, hence it is natural to expect the discretization to produce symmetric matrices. Direct application of the trapezoidal rule leads to nonsymmetric matrices. We can rectify the symmetry issue by simple algebraic manipulations. Obtaining symmetric matrices brings an additional advantage. For example, when the matrices are symmetric, the condition number reduces to the ratio of the maximum and minimum eigenvalues.

We present an instance of the system matrix for each BC considered. For convenience of comparison, we utilize the same kernel function $C(x)$ given in (2.3) with $\delta = 0.5$. In order to demonstrate the algebraic operations needed to obtain a symmetric matrix, we choose $h = \frac{1}{2}$ so that we have small sized system matrices. We start with the periodic BC and see that the corresponding system matrix is not symmetric as seen in the following.

$$A_{\mathtt{p}} = \begin{bmatrix} c-\frac{h}{2} & -\frac{h}{2} & 0 & -\frac{h}{2} & -\frac{h}{2} \\ -\frac{h}{2} & c-h & -\frac{h}{2} & 0 & 0 \\ 0 & -\frac{h}{2} & c-h & -\frac{h}{2} & 0 \\ 0 & 0 & -\frac{h}{2} & c-h & -\frac{h}{2} \\ -\frac{h}{2} & -\frac{h}{2} & 0 & -\frac{h}{2} & c-\frac{h}{2} \end{bmatrix}_{5\times 5.}$$

We can easily obtain a symmetric matrix by applying the BC to the system equations. Namely, by setting $(u_{\mathtt{p}})_1 = (u_{\mathtt{p}})_n$ and $(f_{\mathtt{p}})_1 = (f_{\mathtt{p}})_n$. When we add the last column to the first one, we see that the first and last rows are identical. Using $(f_{\mathtt{p}})_1 = (f_{\mathtt{p}})_n$, we can eliminate the last row because it is identical to the first row. This gives rise to a reduced system matrix of size $(n-1)\times(n-1)$ and the resulting matrix is symmetric.

For the antiperiodic BC, we obtain the following system matrix.

$$A_{\mathtt{a}} = \begin{bmatrix} c-\frac{h}{2} & -\frac{h}{2} & 0 & \frac{h}{2} & \frac{h}{2} \\ -\frac{h}{2} & c-h & -\frac{h}{2} & 0 & 0 \\ 0 & -\frac{h}{2} & c-h & -\frac{h}{2} & 0 \\ 0 & 0 & -\frac{h}{2} & c-h & -\frac{h}{2} \\ \frac{h}{2} & \frac{h}{2} & 0 & -\frac{h}{2} & c-\frac{h}{2} \end{bmatrix}_{5\times 5.}$$

Similar to the periodic BC case, we can obtain a symmetric matrix by applying the BC to the system equations. Namely, by setting $(u_{\mathtt{p}})_1 = -(u_{\mathtt{a}})_n$ and $(f_{\mathtt{a}})_1 = -(f_{\mathtt{a}})_n$. When we subtract the last column from the first one, we see that the first and last rows are identical. Using $(f_{\mathtt{a}})_1 = -(f_{\mathtt{a}})_n$, we can eliminate the last row because it is identical to the first one. This gives rise to a reduced system matrix of size $(n-1)\times(n-1)$ and the resulting matrix is symmetric.

For the Neumann BC, we obtain the following system matrix.

$$A_{\mathtt{N}} = \begin{bmatrix} c-h & -h & 0 & 0 & 0 \\ -\frac{h}{2} & c-h & -\frac{h}{2} & 0 & 0 \\ 0 & -\frac{h}{2} & c-h & -\frac{h}{2} & 0 \\ 0 & 0 & -\frac{h}{2} & c-h & -\frac{h}{2} \\ 0 & 0 & 0 & -h & c-h \end{bmatrix}_{5\times 5.}$$

We multiply the first and last rows by $1/2$ as well the entries $(f_{\mathtt{N}})_1$ and $(f_{\mathtt{N}})_n$. This multiplication operation gives an equivalent system matrix which is symmetric.

For the Dirichlet BC, we obtain the following system matrix.

$$A_{\mathtt{D}} = \begin{bmatrix} c-h & 0 & 0 & 0 & 0 \\ -\frac{h}{2} & c-h & -\frac{h}{2} & 0 & 0 \\ 0 & -\frac{h}{2} & c-h & -\frac{h}{2} & 0 \\ 0 & 0 & -\frac{h}{2} & c-h & -\frac{h}{2} \\ 0 & 0 & 0 & 0 & c-h \end{bmatrix}_{5\times 5.}$$

The values $(u_{\mathtt{D}})_1$ and $(u_{\mathtt{D}})_n$ are known because they are part of the BC. Hence, by deleting the first and last columns as well the first and last rows, we obtain a symmetric system matrix of size $(n-2)\times(n-2)$.

We present the structure of the system matrices. The matrix $A^s_{\mathtt{p}}$ is symmetric positive semidefinite, whereas the matrix $A^s_{\mathtt{a}}$ is symmetric positive definite. Both matrices are of size $(n-1)\times(n-1)$, diagonally dominant, and Toeplitz. For the matrix definition, it is sufficient to provide only the first row due to the Toeplitz property. Assuming $h \leq \delta$, we present the first rows of $A^s_{\mathtt{p}}$ and $A^s_{\mathtt{a}}$ in Figures 3.3 and 3.2, respectively.

The matrix $A^s_{\mathtt{N}}$ is symmetric positive semidefinite and is of size $n \times n$. Whereas the matrix $A^s_{\mathtt{D}}$ is symmetric positive definite and is of size $(n-2)\times(n-2)$. Both matrices are diagonally dominant. Assuming $h \leq \delta$, we present the matrix $A^s_{\mathtt{N}} - cI$ in Figure 3.4 and assuming $2h \leq \delta$, we present the matrix $A^s_{\mathtt{D}} - cI$ in Figure 3.5. In addition, both $A^s_{\mathtt{p}}$ and $A^s_{\mathtt{N}}$ have the zero row sum property.

$$r_{\mathtt{p}} = [c-h,\ \overbrace{-h,\ \cdots,\ -h}^{\frac{\delta}{h}-1},\ \frac{-h}{2},\ 0,\ \cdots,\ 0,\ \frac{-h}{2},\ \overbrace{-h,\ \cdots,\ -h}^{\frac{\delta}{h}-1}]$$

Figure 3.2. The first row of the matrix $A^s_{\mathtt{p}}$.

$$r_{\mathtt{a}} = [c-h,\ \overbrace{-h,\ \cdots,\ -h}^{\frac{\delta}{h}-1},\ \frac{-h}{2},\ 0,\ \cdots,\ 0,\ \frac{h}{2},\ \overbrace{h,\ \cdots,\ h}^{\frac{\delta}{h}-1}]$$

Figure 3.3. The first row of the matrix $A^s_{\mathtt{a}}$.

3.4. Error Analysis

For error analysis, we start with rewriting our operators

$$-\mathcal{C}_{\mathtt{BC}}u := \big(\mathcal{M}_{\mathtt{BC}} - c\big)u,$$

where $\mathtt{BC} = \{\mathtt{p}, \mathtt{a}, \mathtt{N}, \mathtt{D}\}$. The explicit expression of $\mathcal{C}_{\mathtt{BC}}$ is

$$\mathcal{C}_{\mathtt{BC}}u(x) = \int_\Omega K_{\mathtt{BC}}(x,x')u(x')dx'.$$

Since error analysis calls for differentiation, we assume that $u, f \in C^2(\Omega)$. Furthermore, our analysis assumes invertible operators. Since the spectra of the operators $\mathcal{M}_{\mathtt{p}}$ and $\mathcal{M}_{\mathtt{N}}$ contain zero eigenvalues, the error analysis we carry out covers the operators $\mathcal{M}_{\mathtt{a}}$ and $\mathcal{M}_{\mathtt{D}}$. The exact expressions of $\mathcal{C}_{\mathtt{a}}$ and $\mathcal{C}_{\mathtt{D}}$ can be obtained from (2.8) and (2.15), respectively.

The operators $\mathcal{C}_{\mathtt{p}}$ and $\mathcal{C}_{\mathtt{a}}$ are self-adjoint and compact. Since the operators $\mathcal{C}_{\mathtt{N}}$ and $\mathcal{C}_{\mathtt{D}}$ are linear combinations of $\mathcal{C}_{\mathtt{p}}$ and $\mathcal{C}_{\mathtt{a}}$, they are also self-adjoint and compact. We prefer to work with the scaled operators given in the following.

$$\overline{\mathcal{M}}_{\mathtt{BC}}u = \big(I - \overline{\mathcal{C}}_{\mathtt{BC}}\big)u = \overline{f},$$

where I is the identity operator, $\overline{\mathcal{C}}_{\mathtt{BC}} := \frac{1}{c}\mathcal{C}_{\mathtt{BC}}$, and $\overline{f} := \frac{1}{c}f$ for $\mathtt{BC} = \{\mathtt{a}, \mathtt{D}\}$. From (3.21),

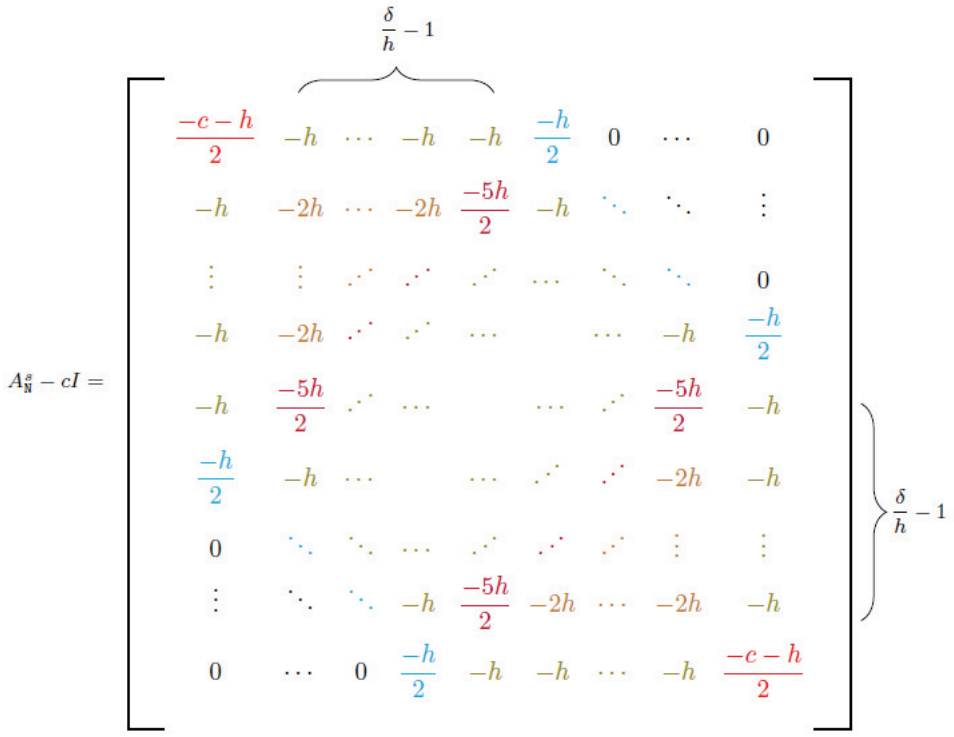

Figure 3.4. Structure of the matrix $A_{\mathtt{N}}^{s}-cI$.

we have

$$\|\overline{\mathcal{C}}_{\mathtt{a}}\| = \frac{\sin(\pi\delta/2)}{\pi\delta/2}.$$

On the other hand, from (3.29), we also have

$$\|\overline{\mathcal{C}}_{\mathtt{D}}\| = \frac{\sin(\pi\delta/2)}{\pi\delta/2}.$$

Consequently, for $\mathtt{BC} = \{\mathtt{a}, \mathtt{D}\}$, we have

$$\|\overline{\mathcal{C}}_{\mathtt{BC}}\| < 1,$$

which indicates that the operators $\overline{\mathcal{C}}_{\mathtt{BC}}$ are contractions. We can conclude that the operators

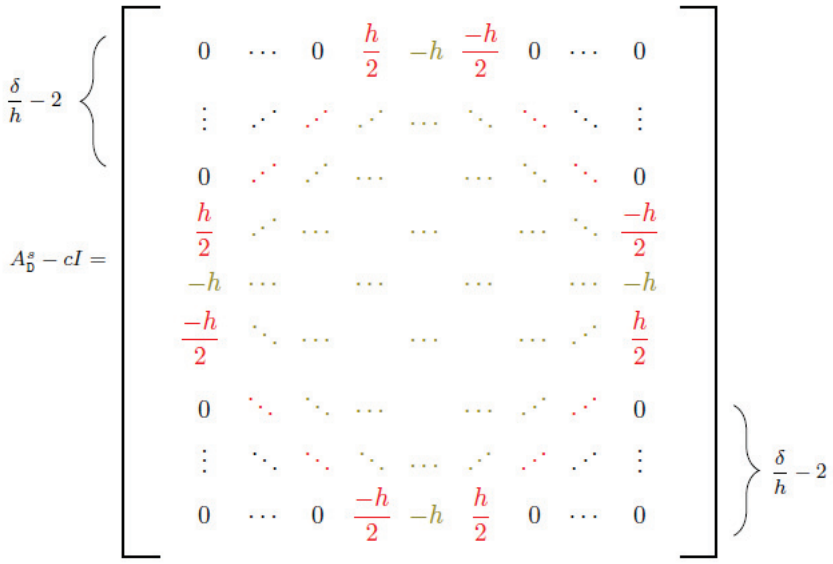

Figure 3.5. Structure of the matrix $A_{\mathrm{D}}^{s}-cI$.

$I-\overline{\mathcal{C}}_{\mathtt{BC}}$ are invertible. It is well known that

$$\|(I-\overline{\mathcal{C}}_{\mathtt{BC}})^{-1}\| \leq \frac{1}{1-\|\overline{\mathcal{C}}_{\mathtt{BC}}\|}. \tag{3.34}$$

From (3.25), we have

$$\frac{1}{1-\frac{\sin(\delta\pi/2)}{\delta\pi/2}} < \frac{64}{\pi^2}\delta^{-2}. \tag{3.35}$$

Hence, combining (3.34) and (3.35), we arrive at

$$\|(I-\overline{\mathcal{C}}_{\mathtt{BC}})^{-1}\| \leq \frac{64}{\pi^2}\delta^{-2}. \tag{3.36}$$

3.4.1. Bounds for the Error

Let us define the sequence of operators

$$\overline{\mathcal{C}}^n_{\mathtt{BC}} u(x) := \sum_{i=1}^{n} \alpha_i K_{\mathtt{BC}}(x_i, x) u(x_i),$$

where α_i denotes the quadrature weight. The operators $\overline{\mathcal{C}}_{\mathtt{BC}}$ are compact. Since the trapezoidal rule is convergent, the sequence $\overline{\mathcal{C}}^n_{\mathtt{BC}}$ is collectively compact and pointwise convergent, i.e., $\overline{\mathcal{C}}^n_{\mathtt{BC}} u \to \overline{\mathcal{C}}_{\mathtt{BC}} u$. A bound for the error can be obtained in the following fashion; see (Kress, 1989, Thm.10.8). For sufficiently large n, more precisely, for all n with

$$\|(I - \overline{\mathcal{C}}_{\mathtt{BC}})^{-1}(\overline{\mathcal{C}}^n_{\mathtt{BC}} - \overline{\mathcal{C}}_{\mathtt{BC}})\overline{\mathcal{C}}^n_{\mathtt{BC}}\| < 1,$$

the solutions to the equations

$$u - \overline{\mathcal{C}}_{\mathtt{BC}} u = \overline{f}, \qquad u_n - \overline{\mathcal{C}}^n_{\mathtt{BC}} u_n = \overline{f}$$

satisfy the following error bound.

$$\|u - u_n\| \leq \|(I - \overline{\mathcal{C}}_{\mathtt{BC}})^{-1}\| \frac{\|(\overline{\mathcal{C}}^n_{\mathtt{BC}} - \overline{\mathcal{C}}_{\mathtt{BC}})\overline{f}\| + \|(\overline{\mathcal{C}}^n_{\mathtt{BC}} - \overline{\mathcal{C}}_{\mathtt{BC}})\overline{\mathcal{C}}^n_{\mathtt{BC}} u\|}{1 - \|(I - \overline{\mathcal{C}}_{\mathtt{BC}})^{-1}(\overline{\mathcal{C}}^n_{\mathtt{BC}} - \overline{\mathcal{C}}_{\mathtt{BC}})\overline{\mathcal{C}}^n_{\mathtt{BC}}\|}. \tag{3.37}$$

A bound for the term $\|(\overline{\mathcal{C}}^n_{\mathtt{BC}} - \overline{\mathcal{C}}_{\mathtt{BC}})\overline{\mathcal{C}}^n_{\mathtt{BC}}\|$ can be given as follows (Atkinson, 1997, (4.1.21)).

$$\|(\overline{\mathcal{C}}^n_{\mathtt{BC}} - \overline{\mathcal{C}}_{\mathtt{BC}})\overline{\mathcal{C}}^n_{\mathtt{BC}}\| \leq c_l \max_{t,s\in\Omega} |E_n(t, s)|,$$

where c_l is a constant and

$$E_n(t,s) := \int_\Omega K_{\mathtt{BC}}(t,v)K_{\mathtt{BC}}(v,s)dv - \sum_{j=1}^{n} \alpha_j K_{\mathtt{BC}}(t,t_j)K_{\mathtt{BC}}(t_j,s)$$

Since the kernel functions under consideration are piecewise constant, the quadrature rule is exact, and hence, $E_n(t,s) = 0$.

The remaining terms in (3.37) are $\|(I - \overline{\mathcal{C}}_{\mathtt{BC}})^{-1}\|$ and $\|(\overline{\mathcal{C}}^n_{\mathtt{BC}} - \overline{\mathcal{C}}_{\mathtt{BC}})\overline{f}\|$. The term $\|(\overline{\mathcal{C}}^n_{\mathtt{BC}} - \overline{\mathcal{C}}_{\mathtt{BC}})\overline{f}\|$ is the quadrature error in the $L^2(\Omega)$-norm. We connect it to the $L^\infty(\Omega)$-norm by using the well-known embedding

$$L^\infty(\Omega) \hookrightarrow L^2(\Omega).$$

Hence,

$$\|(\overline{\mathcal{C}}^n_{\mathtt{BC}} - \overline{\mathcal{C}}_{\mathtt{BC}})\overline{f}\| \leq |\Omega|^{1/2}\|(\overline{\mathcal{C}}^n_{\mathtt{BC}} - \overline{\mathcal{C}}_{\mathtt{BC}})\overline{f}\|_\infty. \tag{3.38}$$

We can quantify the error with the $L^\infty(\Omega)$-norm

$$\|(\overline{\mathcal{C}}^n_{\mathtt{BC}} - \overline{\mathcal{C}}_{\mathtt{BC}})\overline{f}\|_\infty = \frac{2^3 h^2}{12} \max_{x\in\Omega} |\overline{f}''(x)|. \tag{3.39}$$

Consequently, combining (3.38) and (3.39), we obtain

$$\|(\overline{\mathcal{C}}^n_{\mathtt{BC}} - \overline{\mathcal{C}}_{\mathtt{BC}})\overline{f}\| = \mathcal{O}(h^2).$$

To the best of the author's knowledge, the term $\|(I - \overline{\mathcal{C}}_{\mathtt{BC}})^{-1}\|$ can be quantified only by resorting to a discretized form. However, we have an advantage, namely, we have the bound (3.36) at our disposal. Putting all pieces together, we arrive at the error bound

$$\|u - u_n\| = \mathcal{O}(h^2\delta^{-2}).$$

3.4.2. Numerical Tests Verifying the Error Bound

We report the relative error in $L^2(\Omega)$ for varying values of δ when h is fixed and for varying values of h when δ is fixed. We choose the functions $u = \cos(\pi x/2)$ and $u = \sin(x)$ for the antiperiodic and Dirichlet problem, respectively, as the exact solution. We compute the right hand side function f according to given exact solutions. We report the error in Tables 3.1 and 3.2. We observe that the convergence rates are in agreement with our theoretical result.

Table 3.1. Relative errors in L^2-norm for varying h when $\delta = 2^{-4}$.

	$\mathcal{M}_{\mathtt{a}}$	Ratio $\mathcal{M}_{\mathtt{a}}$	$\mathcal{M}_{\mathtt{D}}$	Ratio $\mathcal{M}_{\mathtt{D}}$
$h = 2^{-4}$	0.333655	...	0.027641	...
$h = 2^{-5}$	0.111183	3.00	0.009184	3.00
$h = 2^{-6}$	0.030319	3.66	0.002502	3.64
$h = 2^{-7}$	0.007756	3.93	0.000640	3.90
$h = 2^{-8}$	0.001950	3.97	0.000161	3.97
$h = 2^{-9}$	0.000488	3.99	0.000040	4.02

Table 3.2. Relative errors in L^2-norm for varying δ when $h = 2^{-5}$.

	$\mathcal{M}_{\mathtt{a}}$	Ratio $\mathcal{M}_{\mathtt{a}}$	$\mathcal{M}_{\mathtt{D}}$	Ratio $\mathcal{M}_{\mathtt{D}}$
$\delta = 2^{-5}$	0.333414	...	0.027506	...
$\delta = 2^{-4}$	0.111183	2.99	0.009184	2.99
$\delta = 2^{-3}$	0.030367	3.66	0.002521	3.64
$\delta = 2^{-2}$	0.007814	3.88	0.000662	3.81

3.5. Numerical Experiments

For each BC considered, we compare the condition number of the original continuous operator $\mathcal{M}_{\mathtt{BC}}$ against the discretized operator $A^s_{\mathtt{BC}}$ in the form of a symmetric system matrix. This reduces the condition number of the discretized operator to the ratio of the maximum and minimum eigenvalues.

Table 3.3. Condition number of the periodic operator $\mathcal{M}_{\mathtt{p}}$.

	$\kappa_e(\mathcal{M}_{\mathtt{p}})$	$\frac{7.303}{\pi^2}\delta^{-2}$	$\kappa_e(A^s_{\mathtt{p}})$	$\kappa_e(A^s_{\mathtt{p}})$ rate
$\delta = 2^{-1}$	3.3359	2.9596	3.3358	-
$\delta = 2^{-2}$	12.1609	11.8384	12.1582	3.64
$\delta = 2^{-3}$	47.5941	47.3536	47.5588	3.91
$\delta = 2^{-4}$	190.1750	189.4144	189.2012	3.97
$\delta = 2^{-5}$	760.7300	757.6576	748.6265	3.96

We show the quantifications in Tables 3.3, 3.4, 3.5, and 3.6 for the periodic, antiperiodic, Neumann, and Dirichlet BC, respectively. We use varying values of δ; $\delta = 2^{-j},\ j = 1, \ldots, 5$. We report the condition number values as a function of the δ values.

We know the eigenvalues $\lambda^{\mathtt{p}}_{\min}$ and $\lambda^{\mathtt{a}}_{\min}$ exactly; see (3.14) and (3.21). In fact, for a fixed δ, we can also compute the maximal eigenvalue exactly. Due to the decay of the $\mathrm{sinc}(x)$ function, it is sufficient to check only a certain number of k values to find out $\lambda^{\mathtt{p}}_{\max}$ and $\lambda^{\mathtt{a}}_{\max}$. From (3.3), (3.4), and (3.29), we report the exact value $\kappa(\mathcal{M}_{\mathtt{BC}})$ for fixed δ and report this in the first column in the related tables.

We report the condition number of the matrices $A^s_{\mathtt{p}}$, $A^s_{\mathtt{a}}$, $A^s_{\mathtt{N}}$, and $A^s_{\mathtt{D}}$ (the third column in the related tables) and these figures are computed with the value of $h = 2^{-9}$. In the last column, we report the the growth rate of $\kappa(A^s_{\mathtt{BC}})$ (the fourth column in the related tables) with decreasing δ and clearly see the δ^{-2} behavior with varying δ.

For the case of periodic BC, from (3.17) and (3.18), we know that the coefficient of δ^{-2} lies in interval of $(\frac{6}{\pi^2}, \frac{24}{\pi^2})$. We want to identify this coefficient approximately. Using the improved upper bound we found for (3.15), which is approximately $2.434\,\delta$, we obtain an improved approximate coefficient by employing a perturbation expansion of $\frac{2.434\,\delta}{2\delta - \frac{2\sin(\pi\delta)}{\pi}}$. We conclude that the coefficient is approximately $\frac{7.303}{\pi^2}\delta^{-2}$ and report it (the second column in the related tables) in Table 3.3. In the case of antiperiodic BC, from (3.24) and (3.25), we know that the coefficient of δ^{-2} lies in interval of $(\frac{24}{\pi^2}, \frac{96}{\pi^2})$. In the same way, we conclude that the coefficient is approximately $\frac{29.212}{\pi^2}\delta^{-2}$ and report it in Table 3.4.

For all BC, we see that the condition number of the original continuous operator $\mathcal{M}_{\mathtt{BC}}$ and its discretized counterpart $A^s_{\mathtt{BC}}$ are in good agreement. The condition number clearly depends only on δ and behaves like δ^{-2}.

In Table 3.7, we report the quantification of the condition number of the matrices

Table 3.4. Condition number of the antiperiodic operator $\mathcal{M}_{\mathtt{a}}$.

	$\kappa(\mathcal{M}_{\mathtt{a}})$	$\frac{29.212}{\pi^2}\delta^{-2}$	$\kappa(A^s_{\mathtt{a}})$	$\kappa(A^s_{\mathtt{a}})$ rate
$\delta = 2^{-1}$	11.8384	11.8392	11.8376	-
$\delta = 2^{-2}$	47.6029	47.3568	47.5854	4.02
$\delta = 2^{-3}$	190.1843	189.4272	189.6458	3.99
$\delta = 2^{-4}$	760.3800	757.7088	755.3921	3.98
$\delta = 2^{-5}$	3042.8800	3030.8352	2993.6655	3.96

Table 3.5. Condition number of the Neumann operator $\mathcal{M}_{\mathtt{N}}$.

	$\kappa_e(\mathcal{M}_{\mathtt{N}})$	$\frac{29.212}{\pi^2}\delta^{-2}$	$\kappa_e(A^s_{\mathtt{N}})$	$\kappa_e(A^s_{\mathtt{N}})$ rate
$\delta = 2^{-1}$	12.1610	11.8392	12.2061	-
$\delta = 2^{-2}$	47.6029	47.3568	47.7478	3.91
$\delta = 2^{-3}$	190.1843	189.4272	190.2889	3.99
$\delta = 2^{-4}$	760.7000	757.7088	758.3742	3.99
$\delta = 2^{-5}$	3042.9200	3030.8352	3004.8940	3.96

for different values of h when $\delta = 2^{-2}$. In the last column where we indicate $h \to 0$, we report the exact value $\kappa(\mathcal{M}_{\mathtt{BC}})$ for the choice of $\delta = 2^{-2}$. We observe that of $\kappa(A^s_{\mathtt{BC}})$ approaches to $\kappa(\mathcal{M}_{\mathtt{BC}})$ as $h \to 0$. In addition, when $4h \leq \delta$, there is a mild dependence of $\kappa(A^s_{\mathtt{BC}})$ on h and but the figures are getting closer to $\kappa(\mathcal{M}_{\mathtt{BC}})$ as $h \to 0$.

3.6. Comparison to the Original Peridynamics Operator

We are in a position to make comparison to sharp bounds given in Aksoylu and Unlu (2014). The authors used the discretized form of operator of $\mathcal{L}_{\text{orig}}$, $\mathcal{L}^h_{\text{orig}}$, with non-local homogeneous Dirichlet BC. Linear and constant finite element discretizations were used. The sharp lower bound for $\lambda_{\min}(\mathcal{L}^h_{\text{orig}})$ was more demanding than the upper one. The authors had to exploit sophisticated analysis to find the sharp lower bound. Namely, the nonlocal characterization of Sobolev spaces Bourgain et al. (2001); Ponce (2004) was used to obtain the following bound:

$$\underline{\alpha}\,\delta^3 h \leq \lambda_{\min}(\mathcal{L}^h_{\text{orig}}).$$

Table 3.6. Condition number of the Dirichlet operator $\mathcal{M}_{\mathtt{D}}$.

	$\kappa(\mathcal{M}_{\mathtt{D}})$	$\frac{29.212}{\pi^2}\delta^{-2}$	$\kappa(A^s_{\mathtt{D}})$	$\kappa(A^s_{\mathtt{D}})$ rate
$\delta = 2^{-1}$	12.1610	11.8392	12.1599	-
$\delta = 2^{-2}$	47.6029	47.3568	47.5854	3.91
$\delta = 2^{-3}$	190.1843	189.4272	189.6457	3.99
$\delta = 2^{-4}$	760.7000	757.7088	755.7062	3.98
$\delta = 2^{-5}$	3042.9200	3030.8352	2993.6655	3.96

Table 3.7. Condition number for various h when $\delta = 2^{-2}$.

	$h = \frac{\delta}{2}$	$h = \frac{\delta}{4}$	$h = \frac{\delta}{8}$	$h = \frac{\delta}{16}$	$h = \frac{\delta}{32}$	$h = \frac{\delta}{64}$	$h \to 0$
$\kappa_e(A^s_{\mathtt{p}})$	6.8284	10.0474	11.5724	12.0114	12.1231	12.1511	12.1609
$\kappa(A^s_{\mathtt{a}})$	25.2741	39.2302	45.3704	47.0287	47.4523	47.5587	47.6029
$\kappa_e(A^s_{\mathtt{N}})$	32.1634	43.8623	47.9481	48.3441	48.1095	47.8864	47.6029
$\kappa(A^s_{\mathtt{D}})$	26.2741	39.2302	45.3704	47.0287	47.4523	47.5587	47.6029

For the upper bound, a special function was used together with a Rayleigh quotient argument and the authors obtained

$$\lambda_{\min}(\mathcal{L}^h_{\text{orig}}) \leq \overline{\alpha}\,\delta^3 h.$$

On the other hand, the sharp upper bound for $\lambda_{\max}(\mathcal{L}^h_{\text{orig}})$ was more demanding than the lower one. The authors had to find out explicit expressions of the stiffness matrix entries. Then, an application of the Gershgorin circle theorem was used. Assuming $3h \leq \delta$, the following bound was obtained:

$$\lambda_{\max}(\mathcal{L}^h_{\text{orig}}) \leq \overline{\beta}\,(5\delta h - 6h^2).$$

For the lower bound, a special function was used together with a Rayleigh quotient argument and the authors obtained the same lower bound quantification of

$$\underline{\beta}\,(5\delta h - 6h^2) \leq \lambda_{\max}(\mathcal{L}^h_{\text{orig}}).$$

Here the constants $\underline{\alpha}$, $\overline{\alpha}$, $\underline{\beta}$, and $\overline{\beta}$ are all absolute constants, meaning that they do not have dependence on δ and h. Furthermore, by using numerical linear algebra techniques related to characterization of the minimal eigenvalue of Toeplitz matrices Böttcher and Widom (2007); Kac et al. (1953), the authors identified an asymptotic statement regarding the constant $\underline{\alpha}$. More precisely, as $h \to 0$,

$$\underline{\alpha} \to \frac{3\pi^2}{2}. \tag{3.40}$$

Now, we state our bounds in this thesis from a different perspective. We want to translate the bounds for the condition number into bounds for the extremal eigenvalues. For $\lambda^{\mathtt{p}}_{\max}$ and $\lambda^{\mathtt{a}}_{\max}$, we already have (3.15) and (3.22), respectively. Combining (3.15) with (3.20) and (3.22) with (3.26), we arrive at the following bounds.

$$\frac{\pi^2}{12}\delta^3 < \lambda^{\mathtt{p}}_{\min,2} \qquad\qquad < \frac{\pi^2}{2}\delta^3,$$

$$\frac{\pi^2}{48}\delta^3 < \lambda^{\mathtt{a}}_{\min}, \lambda^{\mathtt{N}}_{\min,2}, \lambda^{\mathtt{D}}_{\min} < \frac{\pi^2}{8}\delta^3.$$

Note that the factor π^2 appears in (3.40). The same factor appears in all minimal eigenvalue bounds for the original continuous operator. This can be interpreted as an indication that the operator $\mathcal{L}^h_{\text{orig}}$ is close to $\mathcal{L}$ when h is small.

CHAPTER 4

CONVERGENCE ANALYSIS OF A MULTIGRID METHOD

We carried out conditioning analysis in Chapter 3 and showed that the original continuous operators have ill-conditioning indicated by δ^{-2}. We numerically showed that as long as the ratio δ/h is big enough (≥ 4), corresponding discrete problems have the same δ^{-2} ill-conditioning. So, it is important to find efficient preconditioners. In this chapter, we propose a multigrid method for systems of equations obtained by discretizing with Nyström method with Trapezoidal rule. We carry out spectral convergence analyses for a two-grid and a multigrid method. We also analyze smoothers. Results of this chapter and more can be found in Aksoylu and Kaya (2018b).

Smoothers are one of the building blocks for multigrid methods. Jacobi methods have been frequently used probably due to their ease of use. Convergence speed of a multigrid method highly depends on the smoother used. So, it is important to obtain effective smoothers for a given problem. In multigrid context, effective smoother means that it enables a fast multigrid convergence. There exist guiding spectral analysis done for 1D elliptic model problem in Briggs et al. (2000); Hackbusch (1985, 2016) to find effective smoothers. The strategy used there is to damp the oscillatory modes effectively, simultaneously. Multigrid method for Fredholm second kind systems (multigrid second kind) dates back to 1970s Hackbusch (1979); Hemker and Schippers (1981); Schippers (Schippers); Hackbusch (1981). However, to do the best of our knowledge, a guiding spectral analysis is still not available for smoothers. Picards' iteration is the most preferred one for Fredholm second kind systems Hackbusch (1985). Because, the operators of the second kind have the smoothing property. Jacobi-like relaxations have been considered wrong choices so far.

In this thesis, we provide spectral analyses using weighted (damped)-Jacobi relaxation to find effective smoothers. We obtain spectrum of system matrices of periodic, antiperiodic and Dirichlet problems using eigenfunctions of original continuous operators. We find the eigenvalues of the matrices in terms of mesh size h and nonlocality parameter δ. Knowing spectrum of a matrix may bring some advantages such as designing effective relaxation schemes. Similarly, one can construct effective smoothers using

spectrum of the matrices which is done for 1D Poisson boundary value problem Briggs et al. (2000); Hackbusch (2016). For a relaxation scheme to be a smoother, it must damp the oscillatory modes effectively. In the light of this fact, we propose two strategies to construct smoothers using weighted Jacobi relaxation. The first strategy depends on the idea that damping the most oscillatory mode as quickly as possible. We find a parameter that carry out this idea for antiperiodic problem for which weighted Jacobi is equivalent to Picards' iteration. This approach shed some light on working principle of Picards' iteration from spectral point of view. The second strategy depends on the idea that damping the oscillatory modes as quickly as possible, simultaneously. This idea has already been applied to 1D Poisson boundary value problem Hackbusch (2016); Briggs et al. (2000). It is not easy to find the optimal parameter algebraicly for this strategy, but we provide a way to find it numerically for given problem parameters. The smoother in the multigrid context has only the purpose to enable a fast multigrid convergence. Based on this fact, we compare relaxation schemes obtained from the two strategies.

4.1. Derivation of Eigenvalues of System Matrices

In this section, we derive eigenvalues of the system matrices $A^s_{\mathtt{BC}}$, $\mathtt{BC} = \{\mathtt{p}, \mathtt{a}, \mathtt{D}\}$. We know that the operators $\mathcal{M}_{\mathtt{BC}}$, $\mathtt{BC} = \{\mathtt{p}, \mathtt{N}\}$ contain zero eigenvalue and hence they are not invertible. Similarly, their corresponding system matrices $A^s_{\mathtt{BC}}$, $\mathtt{BC} = \{\mathtt{p}, \mathtt{N}\}$ contain zero eigenvalue and they are not invertible. So, we will not consider them to find smoothers. However, since the matrix $A^s_{\mathtt{D}}$ assumes eigenvalues of the matrix $A^s_{\mathtt{p}}$, we also show how to derive spectrum of $A^s_{\mathtt{p}}$. We start with the matrix $A^s_{\mathtt{p}}$.

4.1.1. Periodic Matrix $A^s_{\mathtt{p}}$

$A^s_{\mathtt{p}}$ is symmetric, positive semi-definite, Toeplitz matrix. It satisfies zero row sum property and hence has zero eigenvalue. We give its spectrum in Lemma 4.1.1. We find bounds for the spectrum in Lemma 4.1.2

Lemma 4.1.1 *The matrix A^s_{p} assumes the eigenvectors*

$$\mathbf{v}_k^j := \begin{cases} \cos\left(\frac{j(k-1)2\pi}{n-1}\right), & 0 \le j \le n-2, \qquad 1 \le k \le \frac{n+1}{2}, \\ \\ \sin\left(\frac{j(k-1)2\pi}{n-1}\right), & 0 \le j \le n-2, \qquad \frac{n+1}{2} < k \le n-1 \end{cases} \tag{4.1}$$

with the corresponding eigenvalues

$$\left.\begin{aligned} &\lambda_k(A^s_{\mathrm{p}}) := 2\delta + h\cos\left(\delta(k-1)\pi\right) + h - 2h\textstyle\sum_{l=0}^{d}\cos\left(l(k-1)\pi h\right) \\ &= \begin{cases} 0, & k = 1 \\ 2\delta - h\frac{\sin((k-1)\pi\delta)\sin((k-1)\pi h)}{2\sin^2(\frac{(k-1)\pi h}{2})}, & k = 2, ..., n-1. \end{cases} \end{aligned}\right\} \tag{4.2}$$

Recall that $\mathbf{v}_k^j$ denotes the component of the vector $\mathbf{v}_k$.

Proof First, note that, the eigenvectors given in set (4.1) form an orthonormal basis for $\mathbb{R}^{n-1}$, since

$$\mathbf{v}_k.\mathbf{v}_l := \begin{cases} 0, & \text{if} \quad 1 \le k \ne l \le n-1, \\ \\ \frac{n-1}{2}, & \text{if} \quad 2 \le k = l \le n-1, \\ \\ n-1, & \text{if} \quad k = l = 1. \end{cases}$$

So, the set of eigenvectors covers all eigenvalues. Now, we consider the matrix $2\delta I - A^s_{\mathrm{p}}$ which is simpler. To prove the lemma, we show for each k ($k = 1, ..., n-1$) that $\mathbf{r}_{j+1}.\mathbf{v}_k = \lambda_k(2\delta I - A^s_{\mathrm{p}})\mathbf{v}_k^j$ for $j = 0, ..., n-2$. Recall that $\mathbf{r}_j$ is the jth row of the matrix $2\delta I - A^s_{\mathrm{p}}$. Rows of the matrix originate from three different integral equations. First, we consider the rows $\mathbf{r}_j$ for $\delta/h < j < n - \delta/h$. These rows are obtained from the discretization of the following integral equation

$$\int_{x-\delta}^{x+\delta} u(x')dx' = f, \qquad x \in [-1+\delta, 1-\delta]$$

with Trapezoidal rule and imposing periodic boundary condition to the matrix $A_{\mathtt{p}}$. For our purpose, we introduce the operator $\mathtt{Trp}$ which is well known numerical integration with Trapezoidal rule with uniformly distributed nodes. The function v_k stands for the continuous form (eigenfunction of the original continuous operator) of the discrete vector $\mathbf{v}_k$ which is defined as

$$v_k := \begin{cases} \cos((x+1)(k-1)\pi), & 1 \le k \le \frac{n+1}{2}, \\ \\ \sin((x+1)(k-1)\pi), & \frac{n+1}{2} < k \le n-1. \end{cases}$$

Note that, since $e_k^{\mathtt{p}}(x) := e^{i\pi kx}$, $k \in \mathbb{N}$ are eigenfunctions of the operator $\mathcal{M}_{\mathtt{p}}$, $\sin(k\pi x)$ and $\cos(k\pi x)$, $k \in \mathbb{N}$ are also eigenfunctions for $\mathcal{M}_{\mathtt{p}}$. For these rows, we have

$$\left.\begin{array}{l} \mathbf{r}_{j+1}.\mathbf{v}_k = \mathtt{Trp}\left(\int_{x-\delta}^{x+\delta} v_k(x')dx'\right) = \\ \\ h\left(\frac{1}{2}\mathbf{v}_k^{j-\delta/h} + \mathbf{v}_k^{j-\delta/h+1} + ... + \mathbf{v}_k^{j} + ... + \mathbf{v}_k^{j+\delta/h-1} + \frac{1}{2}\mathbf{v}_k^{j+\delta/h}\right), \end{array}\right\} \tag{4.3}$$

$k = 1, ..., n-1$. Using simple trigonometric identities, one can easily show that $\mathbf{r}_{j+1}.\mathbf{v}_k = \lambda_k(2\delta I - A_{\mathtt{p}}^s)\mathbf{v}_k^j$ where

$$\lambda_k(2\delta I - A_{\mathtt{p}}^s) = -h\cos\left(\delta(k-1)\pi\right) - h + 2h\sum_{l=0}^{d}\cos\left(l(k-1)\pi h\right), \quad k = 1, ..., n-1. \tag{4.4}$$

Now, we consider the rows $\mathbf{r}_j$ for $1 \le j \le \delta/h$. For these rows, we have

$$\mathbf{r}_{j+1}.\mathbf{v}_k = \mathtt{Trp}\left(\int_{-1}^{x+\delta} v_k(x')dx'\right) + \mathtt{Trp}\left(\int_{x+2-\delta}^{1} v_k(x')dx'\right), \qquad x \in [-1, -1+\delta).$$

Since $\mathbf{v}_k(x) = \mathbf{v}_k(x+2)$, the change of variable $y' = x' - 2$ in the second integral in

above equation leads to

$$\mathbf{r}_{j+1}.\mathbf{v}_k = \mathtt{Trp}\left(\int_{-1}^{x+\delta} v_k(x')dx'\right) + \mathtt{Trp}\left(\int_{x-\delta}^{-1} v_k(x')dx'\right) = \mathtt{Trp}\left(\int_{x-\delta}^{x+\delta} v_k(x')dx'\right)$$

which is equivalent to Equation (4.3). Hence, we have $\mathbf{r}_{j+1}.\mathbf{v}_k = \lambda_k(2\delta I - A^s_{\mathtt{p}})\mathbf{v}^j_k$ with $\lambda_k(2\delta I - A^s_{\mathtt{p}})$ defined in (4.4). Finally, we consider the rows $\mathbf{r}_j$, $n - \delta/h < j \leq n-1$. For these rows, we have

$$\mathbf{r}_{j+1}.\mathbf{v}_k = \mathtt{Trp}\left(\int_{-1}^{x-2+\delta} v_k(x')dx'\right) + \mathtt{Trp}\left(\int_{x-\delta}^{1} v_k(x')dx'\right), \qquad x \in (1-\delta, 1].$$

Since $\mathbf{v}_k(x) = \mathbf{v}_k(x+2)$, the change of variable $y' = x' + 2$ in the first integral in above equation leads to

$$\mathbf{r}_{j+1}.\mathbf{v}_k = \mathtt{Trp}\left(\int_{1}^{x+\delta} v_k(x')dx'\right) + \mathtt{Trp}\left(\int_{x-\delta}^{1} v_k(x')dx'\right) = \mathtt{Trp}\left(\int_{x-\delta}^{x+\delta} v_k(x')dx'\right)$$

which is equivalent to Equation (4.3). Hence, we have $\mathbf{r}_{j+1}.\mathbf{v}_k = \lambda_k(2\delta I - A^s_{\mathtt{p}})\mathbf{v}^j_k$ with $\lambda_k(2\delta I - A^s_{\mathtt{p}})$ defined in (4.4).

Hence, we can conclude that, the matrix $A^s_{\mathtt{p}}$ assumes the eigenvectors in (4.1) with the corresponding eigenvalues in (4.2).

□

Lemma 4.1.2 *The bounds*

$$0 \leq \lambda_k(A^s_{\mathtt{p}}) < 4\delta - 2h$$

hold for $k = 1, 2, ..., n-1$.

Proof It is clear that $\lambda_1(A^s_{\mathtt{p}}) = 0$. Since $\cos(l(k-1)\pi h) \leq 1$ for all l, k and h, from definition of $\lambda_k(A^s_{\mathtt{p}})$ in (4.2), it follows that $\lambda_k(A^s_{\mathtt{p}}) \geq 0$ for $k = 1, ..., n-1$. We show the upper bound by induction. For $k = 1$, it is clear. Let $\delta = dh$ where $d \geq 1$. Then, We show that

$$\lambda_k(A^s_{\mathsf{p}}) = 2\delta - h\sin(k\pi\delta)\cot(k\pi h/2) < 4\delta - 2h, \qquad k = 2, ..., n-1.$$

The above inequality is equivalent to showing that

$$\sin(k\pi dh)\cot(k\pi h/2) > 2 - 2d.$$

First, we show for $d = 1$, i.e.

$$\sin(k\pi h)\cot(k\pi h/2) > 0. \tag{4.5}$$

It is clear that $\sin(k\pi h) > 0$ and $\cot(k\pi h/2) > 0$ for $k = 2, ..., n-1$. Hence, it is true for $d = 1$. Now, assume that

$$\sin(k\pi mh)\cot(k\pi h/2) > 2 - 2m, \qquad k = 2, ..., n-1. \tag{4.6}$$

holds for $m > 1$. We will show that it is true for $d = m + 1$. Using the inequalities (4.5), (4.6) and the fact that $\cos(x) \leq 1$, we arrive at

$$\sin(k\pi(m+1)h)\cot(k\pi h/2) = \sin(k\pi hm)\cos(k\pi h)\cot(k\pi h/2)$$

$$+ \sin(k\pi h)\cos(k\pi hm)\cot(k\pi h/2) \geq \sin(k\pi hm)\cot(k\pi h/2)$$

$$+ \sin(k\pi h)\cot(k\pi h/2) > 2 - 2m + 0 > 2 - 2(m+1).$$

This completes the proof. □

4.1.2. Antiperiodic Matrix A^s_{a}

A^s_{a} is symmetric, positive definite, Toeplitz matrix. We give the eigenvalues in Lemma 4.1.3. We find bounds for the spectrum in Lemma 4.1.4.

Lemma 4.1.3 *The matrix A^s_{a} assumes the eigenvectors*

$$\mathbf{v}_k^j := \begin{cases} \cos\left(\frac{j(k-\frac{1}{2})2\pi}{n-1}\right), & 0 \le j \le n-2, \qquad 1 \le k < \frac{n+1}{2}, \\ \\ \sin\left(\frac{j(k-\frac{1}{2})2\pi}{n-1}\right), & 0 \le j \le n-2, \qquad \frac{n+1}{2} \le k \le n-1 \end{cases} \tag{4.7}$$

with the corresponding eigenvalues

$$\left.\begin{array}{l} \lambda_k(A^s_{\mathsf{a}}) = 2\delta + h\cos\left(\delta\left(k-\frac{1}{2}\right)\pi\right) + h - 2h\sum_{l=0}^{d}\cos\left(l\left(k-\frac{1}{2}\right)\pi h\right) \\ \\ = 2\delta - h\frac{\sin\left(\left(k-\frac{1}{2}\right)\pi\delta\right)\sin\left(\left(k-\frac{1}{2}\right)\pi h\right)}{2\sin^2\left(\frac{\left(k-\frac{1}{2}\right)\pi h}{2}\right)}, \qquad k = 1, ..., n-1. \end{array}\right\} \tag{4.8}$$

Recall that $\mathbf{v}_k^j$ denotes the component of the vector $\mathbf{v}_k$.

Proof First, note that, the eigenvectors given in set (4.7) form an orthonormal basis for $\mathbb{R}^{n-1}$, since

$$\mathbf{v}_k.\mathbf{v}_l := \begin{cases} 0, & \text{if} \quad 1 \le k \ne l \le n-1, \\ \\ \frac{n-1}{2}, & \text{if} \qquad 1 \le k = l \le n-1. \end{cases}$$

So, the set covers all eigenvalues. For simplicity, we consider the matrix $2\delta I - A^s_{\mathsf{a}}$. As in the periodic case, rows of the matrix $2\delta I - A^s_{\mathsf{a}}$ originates from three different integral equations which are given in (2.9). We apply the same procedure in Lemma 4.1.1.

□

Lemma 4.1.4 *The following bounds*

$$0 < \lambda_k(A^s_{\mathsf{a}}) < 4\delta - 2h$$

hold for $k = 1, ..., n-1$.

Proof Since $0 < (k - \frac{1}{2})\pi h < 2\pi$ for $k = 1, 2, ..., n-1$, the terms $\cos\left(l\left(k - \frac{1}{2}\right)\pi h\right)$, $k = 1, ..., n-1$ in (4.8) can not be equal to 1 for a fixed k, simultaneously. So,

$$\lambda_k(A^s_{\mathtt{a}}) > 2\delta + h + h - 2h(\frac{\delta}{h} + 1) = 0.$$

Applying the same steps in Lemma 4.1.2, we can show that

$$\lambda_k(A^s_{\mathtt{a}}) < 4\delta - 2h.$$

□

4.1.3. Dirichlet Matrix $A^s_{\mathtt{D}}$

$A^s_{\mathtt{D}}$ is symmetric, positive definite matrix. Unlike the matrices $A^s_{\mathtt{p}}$ and $A^s_{\mathtt{a}}$, it is not Toeplitz. We give its eigenvalues in Lemma 4.1.5.

Lemma 4.1.5 *The matrix $A^s_{\mathtt{D}}$ assumes the eigenvectors*

$$\mathbf{v}^j_k := \begin{cases} \sin\left(\frac{jk2\pi}{n-1}\right), & 1 \le j \le n-2, \quad 1 \le k < \frac{n-1}{2}, \\ \sin\left(\frac{j(k+\frac{1}{2})2\pi}{n-1}\right), & 1 \le j \le n-2, \quad \frac{n-1}{2} \le k \le n-2 \end{cases} \tag{4.9}$$

with the corresponding eigenvalues

$$\lambda_k(A^s_{\mathtt{D}}) :=$$

$$\begin{cases} 2\delta + h\cos(\delta k\pi) + h - 2h\sum_{l=0}^{d}\cos(lk\pi h), & 1 \le k < \frac{n-1}{2} \\ 2\delta + h\cos\left(\delta\left(k+\frac{1}{2}\right)\pi\right) + h - 2h\sum_{l=0}^{d}\cos\left(l\left(k+\frac{1}{2}\right)\pi h\right), & \frac{n-1}{2} \le k \le n-2. \end{cases}$$

$$= \begin{cases} 2\delta - h\frac{\sin(k\pi\delta)\sin(k\pi h)}{2\sin^2(\frac{k\pi h}{2})}, & 1 \leq k < \frac{n-1}{2} \\ \\ 2\delta - h\frac{\sin\left(\left(k+\frac{1}{2}\right)\pi\delta\right)\sin\left(\left(k+\frac{1}{2}\right)\pi h\right)}{2\sin^2\left(\frac{\left(k+\frac{1}{2}\right)\pi h}{2}\right)}, & \frac{n-1}{2} \leq k \leq n-2. \end{cases} \tag{4.10}$$

Proof First, note that, the eigenvectors given in set (4.9) form an orthonormal basis for $\mathbb{R}^{n-2}$, since

$$\mathbf{v}_k.\mathbf{v}_l := \begin{cases} 0, & \text{if} \quad 1 \leq k \neq l \leq n-2, \\ \\ \frac{n-1}{2}, & \text{if} \quad 1 \leq k = l \leq n-2. \end{cases}$$

So, the set covers all eigenvalues. We consider the matrix $2\delta I - A^s_{\mathtt{D}}$. As before, rows of the matrix $2\delta I - A^s_{\mathtt{D}}$ originates from three different integral equation which are given in (2.16). The rows $\mathbf{r}_j$, $\frac{\delta}{h} < j < n-2-\frac{\delta}{h}$ correspond to bulk of the domain and all operators are same there. In this case,

$$v_k := \begin{cases} \sin((x+1)k\pi), & 1 \leq k < \frac{n-1}{2}, \\ \\ \sin((x+1)(k+\frac{1}{2})\pi), & \frac{n-1}{2} \leq k \leq n-2. \end{cases}$$

Since $v_k(0) = v_k(2) = 0$, we have

$$\mathbf{r}_{j+1}.\mathbf{v}_k = \mathtt{Trp}\left(\int_{x-\delta}^{x+\delta} v_k(x')dx'\right), \qquad k = 1, ..., n-2. \tag{4.11}$$

We know from periodic and antiperiodic matrices that $\mathbf{r}_{j+1}.\mathbf{v}_k = (2\delta - \lambda_k)\mathbf{v}_k^j$ where λ_k is defined in (4.10). We consider the first δ/h rows which are obtained by discretization of the integrals in the first line of equation (2.16). Since $v_k(0) = v_k(2) = 0$, we have

$$\mathbf{r}_{j+1}.\mathbf{v}_k = \mathtt{Trp}\left(\int_{-1}^{x+\delta} v_k(x')dx'\right) - \mathtt{Trp}\left(\int_{-1}^{-x+\delta-2} v_k(x')dx'\right), \quad x \in [-1, -1+\delta).$$

Using the equality $\mathbf{v}_k(-x) = -\mathbf{v}_k(x)$ and doing the change of variable $x^{'} = -y - 2$ in the second integral in above equation we get

$$\mathbf{r}_{j+1}.\mathbf{v}_k = \mathtt{Trp}\left(\int_{-1}^{x+\delta} v_k(x')dx'\right) + \mathtt{Trp}\left(\int_{x-\delta}^{-1} v_k(x')dx'\right) = \mathtt{Trp}\left(\int_{x-\delta}^{x+\delta} v_k(x')dx'\right).$$

The above equation is same with Equation (4.11). Hence, $\mathbf{r}_{j+1}.\mathbf{v}_k = (2\delta - \lambda_k)\mathbf{v}_k^j$ where λ_k is defined in (4.10).

The last δ/h rows are obtained by discretization of the integrals in the third line of equation (2.16). Since $v_k(0) = v_k(2) = 0$, we have

$$\mathbf{r}_{j+1}.\mathbf{v}_k = -\mathtt{Trp}\left(\int_{-x-\delta+2}^{1} v_k(x')dx'\right) + \mathtt{Trp}\left(\int_{x-\delta}^{1} v_k(x')dx'\right), \qquad x \in (1-\delta, 1].$$

Using the equality $\mathbf{v}_k(-x) = -\mathbf{v}_k(x)$ and doing the change of variable $x^{'} = 2 - y$ in the first integral in the above equation, we get

$$\mathbf{r}_{j+1}.\mathbf{v}_k = \mathtt{Trp}\left(\int_{1}^{x+\delta} v_k(x')dx'\right) + \mathtt{Trp}\left(\int_{x-\delta}^{1} v_k(x')dx'\right) = \mathtt{Trp}\left(\int_{x-\delta}^{x+\delta} v_k(x')dx'\right).$$

The above equation is same with Equation (4.11). Hence, $\mathbf{r}_{j+1}.\mathbf{v}_k = (2\delta - \lambda_k)\mathbf{v}_k^j$ where λ_k is defined in (4.10).

□

4.2. Construction of Smoothers for Nonlocal Problems

We start this section by reviewing some basic concepts from Briggs et al. (2000). We consider the linear system of equation

$$A^s_{\mathtt{BC}}\mathbf{u} = \mathbf{f} \tag{4.12}$$

where $\mathtt{BC} = \{\mathtt{a}, \mathtt{D}\}$. These systems have unique solutions. $\mathbf{u}$ always denotes the exact solution of this system and $\mathbf{v}$ denotes an approximation to the exact solution. There are

two ways to measure how well $\mathbf{v}$ approximates $\mathbf{u}$. One is the `error` (or algebraic error) which is simply

$$\mathbf{e} = \mathbf{u} - \mathbf{v}.$$

Unfortunately, the error can be computed only when the exact solution is known. The second way is to compute `residual` which is simply given by

$$\mathbf{r} = \mathbf{f} - A^s_{\mathtt{BC}}\mathbf{v}.$$

By the uniqueness of the solution, $\mathbf{r} = 0$ if and only if $\mathbf{e} = 0$. Using the definitions of $\mathbf{r}$ and $\mathbf{e}$, we can derive the following relation

$$A^s_{\mathtt{BC}}\mathbf{e} = \mathbf{r}$$

between the error and the residual. The above equation is called *residual equation*. In multigrid methods, the residual equation is very important.

We now examine the stationary relaxation schemes for our model problems (4.12). Stationary relaxation methods are not used to approximate the solution of Fredholm second kind systems because the system matrices are generally far from being diagonally dominant. However, they can be used as smoothers for multigrid methods.

As in Briggs et al. (2000), we start with Jacobi relaxation. Since the matrix $A^s_{\mathtt{a}}$ is diagonally constant, we continue with this. Because, this property allows us to obtain eigenvalues of the iteration matrix, explicitly. We express the Jacobi relaxation in matrix form. To do this, we split the matrix $A^s_{\mathtt{a}}$ in the following form

$$A^s_{\mathtt{a}} = D_{\mathtt{a}} - L_{\mathtt{a}} - U_{\mathtt{a}},$$

where $D_{\mathtt{a}}$ corresponds to diagonal of $A^s_{\mathtt{a}}$ and $-L_{\mathtt{a}}$ and $-U_{\mathtt{a}}$ are strictly lower triangular and upper triangular parts of $A^s_{\mathtt{a}}$, respectively. With some algebraic manipulations, $A^s_{\mathtt{a}}\mathbf{u} =$

$\mathbf{f}$ becomes

$$\mathbf{u} = D_{\mathtt{a}}^{-1}(D_{\mathtt{a}} - A_{\mathtt{a}}^{s})\mathbf{u} + D_{\mathtt{a}}^{-1}\mathbf{f} = (I - D_{\mathtt{a}}^{-1}A_{\mathtt{a}}^{s})\mathbf{u} + D_{\mathtt{a}}^{-1}\mathbf{f}.$$

We define the Jacobi iteration matrix by

$$R_{\mathtt{a}}^{j} = (I - D_{\mathtt{a}}^{-1}A_{\mathtt{a}}^{s}).$$

Then, we can define the Jacobi relaxation in matrix form as

$$\mathbf{v}^{1} = R_{\mathtt{a}}^{j}\mathbf{v}^{0} + D_{\mathtt{a}}^{-1}\mathbf{f}.$$

A slight modification of Jacobi relaxation gives weighted (damped) Jacobi relaxation in the matrix form as

$$\mathbf{v}^{1} = [(1-w)I + wR_{\mathtt{a}}^{j}]\mathbf{v}^{0} + wD_{\mathtt{a}}^{-1}\mathbf{f}.$$

If we introduce the weighted Jacobi iteration matrix as

$$R_{\mathtt{a}}^{w} = (1-w)I + wR_{\mathtt{a}}^{j}$$

then the method becomes

$$\mathbf{v}^{1} = R_{\mathtt{a}}^{w}\mathbf{v}^{0} + wD_{\mathtt{a}}^{-1}\mathbf{f}.$$

Since the main diagonal of the matrix $A_{\mathtt{a}}^{s}$ consists of $2\delta - h$, we give the eigenvalues of the iteration matrices $R_{\mathtt{a}}^{j}$ and $R_{\mathtt{a}}^{w}$ by

$$\lambda_k(R_{\mathtt{a}}^j) = \left(1 - \frac{1}{2\delta - h}\lambda_k(A_{\mathtt{a}}^s)\right),$$

$$\lambda_k(R_{\mathtt{a}}^w) = 1 - w + w\lambda_k(R_{\mathtt{a}}^j).$$

It follows from the Lemma 4.1.4 that $\rho(R_{\mathtt{a}}^j) < 1$ and $\rho(R_{\mathtt{a}}^w) < 1$. Hence, Jacobi and weighted Jacobi relaxations converge for $0 < w \leq 1$.

Let $\mathbf{e}^0$ be the initial error in the inital guess. Then, we can represent $\mathbf{e}^0$ in terms of eigenvectors of $A_{\mathtt{a}}^s$ in the form

$$\mathbf{e}^0 = \sum_{k=1}^{n-1} c_k \mathbf{v_k}.$$

The eigenvectors are also called Fourier modes. We know that after m sweeps, the error becomes

$$\mathbf{e}^m = (R_{\mathtt{a}}^w)^m \mathbf{e}^0.$$

From the eigenvector expansion of $\mathbf{e}^0$, we get

$$\mathbf{e}^m = R_{\mathtt{a}}^w \mathbf{e}^0 = \sum_{k=1}^{n-1} c_k (R_{\mathtt{a}}^w)^m \mathbf{v_k} = \sum_{k=1}^{n-1} c_k \lambda_k^m (R_{\mathtt{a}}^w) \mathbf{v_k}.$$

Here, we note that eigenvectors of $A_{\mathtt{a}}^s$ are also eigenvectors for the iteration matrix $R_{\mathtt{a}}^w$. This expansion says that after m iterations, the kth mode of the initial error has been reduced by a factor of $\lambda_k^m(R_{\mathtt{a}}^w)$.

The Fourier modes in the first quarter and last quarter of the spectrum, with wavenumbers in the ranges $1 \leq k \leq \frac{n-1}{4}$, $\frac{3(n-1)}{4} < k \leq n-1$ are called low-frequency or smooth modes. The modes at the center of the spectrum , with wavenumbers in the range $\frac{n-1}{4} < k \leq \frac{3(n-1)}{4}$ are called high-frequency or oscillatory modes.

Having said these, we start analyzing weighted Jacobi relaxation. We aim to find

best choice of w. Notice that

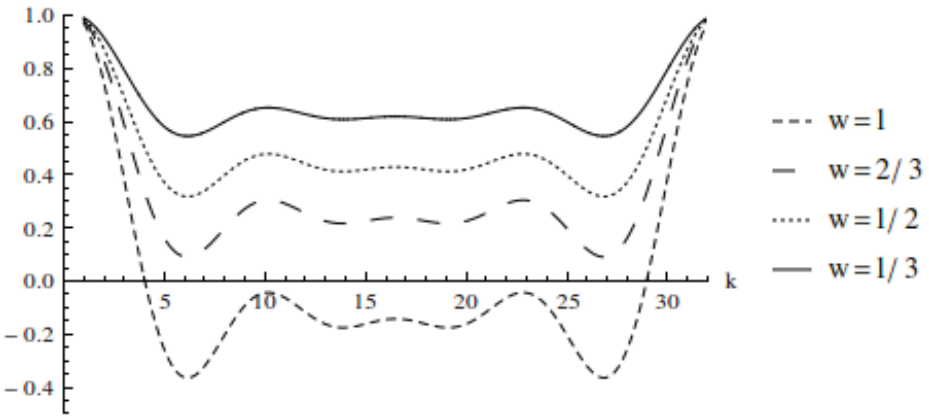

Figure 4.1. Eigenvalues of the iteration matrix R_{a}^w for $w = 1, 2/3, 1/2, 1/3$ for $n = 33$ and $\delta = 0.25$. We assume that eigenvalues are continuous in k.

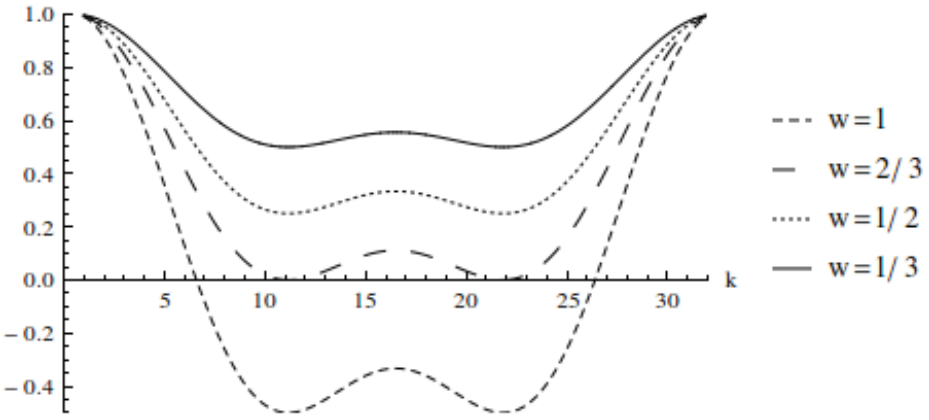

Figure 4.2. Eigenvalues of the iteration matrix R_{a}^w for $w = 1, 2/3, 1/2, 1/3$ for $n = 33$ and $\delta = 0.125$. We assume that eigenvalues are continuous in k.

$$\lambda_1(A_{\mathsf{a}}^s) = \lambda_{n-1}(A_{\mathsf{a}}^s) = \frac{\pi^2\delta^3}{6} + \frac{\pi^2\delta h^2}{12} + \mathcal{O}(h\delta^4) + \mathcal{O}(h^4).$$

Since $\delta > h$, the term $\frac{\pi^2\delta^3}{6}$ dominates and $\lambda_1(A_{\mathsf{a}}^s)$ and $\lambda_{n-1}(A_{\mathsf{a}}^s)$ behaves like $\frac{\pi^2\delta^3}{6}$. It follows from these observations that for all values of w satisfying $0 < w \leq 1$, $\lambda_1(R_{\mathsf{a}}^w)$ and $\lambda_{n-1}(R_{\mathsf{a}}^w)$ behaves like

$$1 - w\frac{\pi^2\delta^3}{6(2\delta - h)}.$$

We infer that δ is the determinant in these eigenvalues. Furthermore, the smaller δ and h are, the closer $\lambda_1(R_{\mathtt{a}}^w)$ and $\lambda_{n-1}(R_{\mathtt{a}}^w)$ are to 1. These show that eigenvalues $\lambda_1(R_{\mathtt{a}}^w)$ and $\lambda_{n-1}(R_{\mathtt{a}}^w)$ which are associated with smoothest modes are always close to 1. This means that, no value of w will damp the smooth components of the error quickly. In Figure 4.1 and 4.2, we present the eigenvalues of the iteration matrix $R_{\mathtt{a}}^w$ for $w = 1, 2/3, 1/2, 1/3$ when $\delta = 0.25$ and $\delta = 0.125$, respectively.

Having observed that no value of w reduces the smooth components effectively, we try to find values of w that reduces oscillatory modes effectively. To accomplish this, we propose two strategies.

4.2.1. The First Strategy

In the first strategy, we just focus on the most oscillatory mode. We aim to damp it as quickly as possible. To do so, we try to minimize the absolute value of eigenvalue of $R_{\mathtt{a}}^w$ corresponding to the most oscillatory mode. We could do this by imposing

$$\lambda_{\frac{n-1}{2}+\frac{1}{2}}(R_{\mathtt{a}}^w) = 0.$$

In order to do this, we assume that $\lambda_k(R_{\mathtt{a}}^w)$ is continuous in k. Lemma 4.2.1 leads to the value

$$w = 1 - \frac{h}{c} = 1 - \frac{h}{2\delta}.$$

Lemma 4.2.1 *Assume that $\lambda_k(R_{\mathtt{a}}^w)$ is continuous in k. Then, $\lambda_{\frac{n}{2}}(R_{\mathtt{a}}^w) = 0$ implies*

$$w = 1 - \frac{h}{2\delta}.$$

Proof We have two cases. First, we assume that δ/h is an odd integer. Then,

$$\lambda_{\frac{n}{2}}(R_{\mathtt{a}}^{w}) = 1 - w + w\left(1 - \frac{2\delta + h\cos\left(\frac{\delta\pi}{h}\right) + h - 2h\sum_{l=0}^{d}\cos(l\pi)}{2\delta - h}\right)$$

$$= 1 - w + w\left(\frac{2\delta - h - 2\delta - h\cos\left(\frac{\delta\pi}{h}\right) - h}{2\delta - h}\right) = 0.$$

Solving for w, we get

$$w = \frac{1}{1 + \frac{2h + h\cos\left(\frac{\delta\pi}{h}\right)}{2\delta - h}} = 1 - \frac{h}{2\delta}.$$

Now, assume that δ/h is an even integer. Then

$$\lambda_{\frac{n}{2}}(R_{\mathtt{a}}^{w}) = 1 - w + w\left(\frac{-h\cos\left(\frac{\delta\pi}{h}\right)}{2\delta - h}\right) = 0.$$

This implies that

$$w = \frac{1}{1 + \frac{h\cos\left(\frac{\delta\pi}{h}\right)}{2\delta - h}} = 1 - \frac{h}{2\delta}.$$

□

We present the eigenvalues of $R_{\mathtt{a}}^{w}$ for $\delta = 0.5, 0.25, 0.125$ when $w = 1 - \frac{h}{2\delta}$ and $n = 33$ in Figure 4.3. The results show that the eigenvalue associated to the most oscillatory mode is very close to 0. Beside this, eigenvalues associated to oscillatory modes (those with $\frac{n-1}{4} < k \leq \frac{3(n-1)}{4}$) are also close to 0. This says that for $w = 1 - \frac{h}{2\delta}$, although smooth component of the error reduced slowly, oscillatory components are damped rapidly for any δ satisfying $0 < \delta < 1$. At this point, we remind the weighted Jacobi relaxation:

$$\mathbf{v}^{1} = R_{\mathtt{a}}^{w}\mathbf{v}^{0} + wD_{\mathtt{a}}^{-1}\mathbf{f} = \left((1-w)I + w(I - D_{\mathtt{a}}^{-1}A_{\mathtt{a}}^{s})\right)\mathbf{v}^{0} + wD_{\mathtt{a}}^{-1}\mathbf{f}.$$

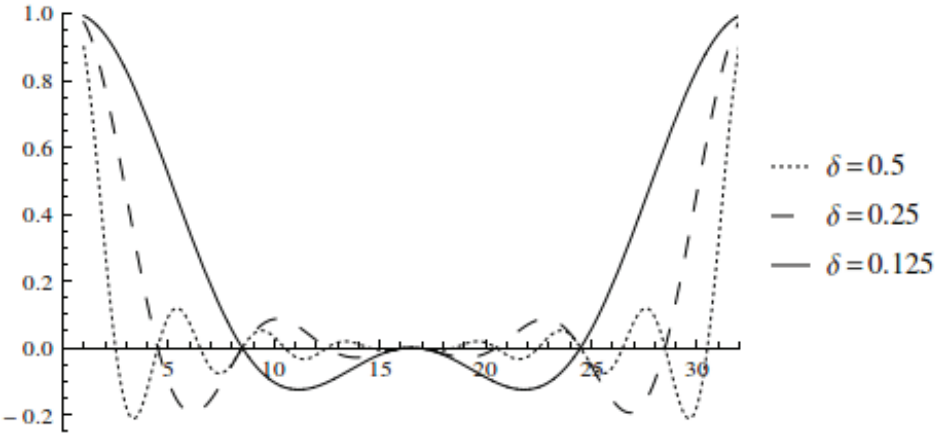

Figure 4.3. Eigenvalues of the iteration matrix $R_{\mathtt{a}}^{w}$ for $\delta = 0.5, 0.25, 0.125$ when $w = 1 - \frac{h}{2\delta}$ and $n = 33$. We assume that eigenvalues are continuous in k.

Substituting $w = 1 - \frac{h}{2\delta}$ into the above equation, weighted Jacobi relaxation turns into

$$\mathbf{v}^1 = \left((1 - 1 + \frac{h}{2\delta})I + (1 - \frac{h}{2\delta})(I - D_{\mathtt{a}}^{-1} A_{\mathtt{a}}^{s}) \right) \mathbf{v}^0 + (1 - \frac{h}{2\delta}) D_{\mathtt{a}}^{-1} \mathbf{f}$$

$$= \left(I - \frac{1}{2\delta} A_{\mathtt{a}}^{s} \right) \mathbf{v}^0 + \frac{1}{2\delta} \mathbf{f}.$$

The above iteration is nothing but Picards' iteration. That is, for $w = 1 - \frac{h}{2\delta}$, the weighted Jacobi is equivalent to Picards' iteration. Picards' iteration is proposed as smoother by Hackbusch for Fredolm second kind systems in his books Hackbusch (1985, 2016).

Now, we examine the Dirichlet matrix $A_{\mathtt{D}}^{s}$. Notice that the main diagonal of $A_{\mathtt{D}}^{s}$ is not constant. So, it is difficult to apply a direct method as we did for $A_{\mathtt{a}}^{s}$. But, if we set the diagonal matrix to $D_{\mathtt{D}} = (2\delta - h)I$ in the splitting $A_{\mathtt{D}}^{s} = D_{\mathtt{D}} + L_{\mathtt{D}} + U_{\mathtt{D}}$, everthing works we did for $A_{\mathtt{a}}^{s}$. Instead, we examine Picards' iteration because it would be interesting to show that the eigenvalue distribution is consistent with the aim of the first strategy. Picards' iteration is given by

$$\mathbf{v}^1 = \left(I - \frac{1}{2\delta} A_{\mathtt{D}}^{s} \right) \mathbf{v}^0 + \frac{1}{2\delta} \mathbf{f}.$$

Eigenfunctions of the matrix $A^s_{\mathtt{D}}$ behave similarly with the eigenfunctions of the matrix $A^s_{\mathtt{a}}$. That is the modes in the range $1 \leq k \leq \frac{n-1}{4}$ and $\frac{3(n-1)}{4} \leq k \leq n-2$ are smooth modes. The modes in the range $\frac{n-1}{4} < k < \frac{3(n-1)}{4}$ are oscillatory modes.

Having said this, we define the iteration matrix by $R^p_{\mathtt{D}} = I - \frac{1}{2\delta} A^s_{\mathtt{D}}$. It is clear that

$$\lambda_k(R^p_{\mathtt{D}}) = 1 - \frac{1}{2\delta}\lambda_k(A^s_{\mathtt{D}}), \qquad k = 1, 2, ..., n-2.$$

The matrix $A^s_{\mathtt{D}}$ assumes all eigenvalues of the matrix $A^s_{\mathtt{a}}$ and $A^s_{\mathtt{p}}$ except $\lambda_1(A^s_{\mathtt{p}}) = 0$. From Lemma 4.1.4, 4.1.2, it follows that

$$\rho(R^p_{\mathtt{D}}) < 1.$$

This says that Picards' iteration converges. Notice that $\lambda_1(A^s_{\mathtt{D}})$ behaves like $\frac{\pi^2\delta^3}{3}$ and $\lambda_{n-2}(A^s_{\mathtt{D}}) = \lambda_{n-1}(A^s_{\mathtt{a}})$ behaves like $\frac{\pi^2\delta^3}{6}$. It follows that $\lambda_1(R^p_{\mathtt{D}})$ behaves like $1 - \frac{\pi^2\delta^2}{6}$ and $\lambda_{n-2}(R^p_{\mathtt{D}})$ behaves like $1 - \frac{\pi^2\delta^2}{12}$. It is easy to show that $\lambda_{\frac{n-1}{2}}(A^s_{\mathtt{p}}) = 2\delta$. From the definitions of $A^s_{\mathtt{D}}$, we can infer that $\lambda_{\frac{n-1}{2}-1}(A^s_{\mathtt{D}})$ and $\lambda_{\frac{n-1}{2}}(A^s_{\mathtt{D}})$ are close to 2δ. Hence, $\lambda_{\frac{n-1}{2}}(R^p_{\mathtt{D}})$ and $\lambda_{\frac{n-1}{2}-1}(R^p_{\mathtt{D}})$ are close to 0. These observations show that eigenvalues associated to smooth modes are always close to 1. Eigenvalues which correspond to two most oscillatory modes are very close to 0. We show eigenvalues of $R^p_{\mathtt{D}}$ in Figure 4.4 for $\delta = 0.5, 0.25, 0.125$ when $n = 33$. This verifies that the working principle behind Picards' iteration is same with the idea of the first strategy. That is, Picards' iteration focus on the most oscillatory mode and aims to damp it effectively.

4.2.2. The Second Strategy

In this strategy, we focus on the oscillatory modes of the iteration matrix of the weighted Jacobi relaxation. Our aim is to damp them effectively, simultaneously. Eigenvalues corresponding to oscillatory modes take place at the center of the spectrum. Actually, this is the strategy applied for 1D Poisson equation Briggs et al. (2000); Hackbusch (1985). For this strategy, it is difficult to find a parameter for the weighted Joacobi, algebraicly, but we provide a way to find an optimal parameter numerically for given problem

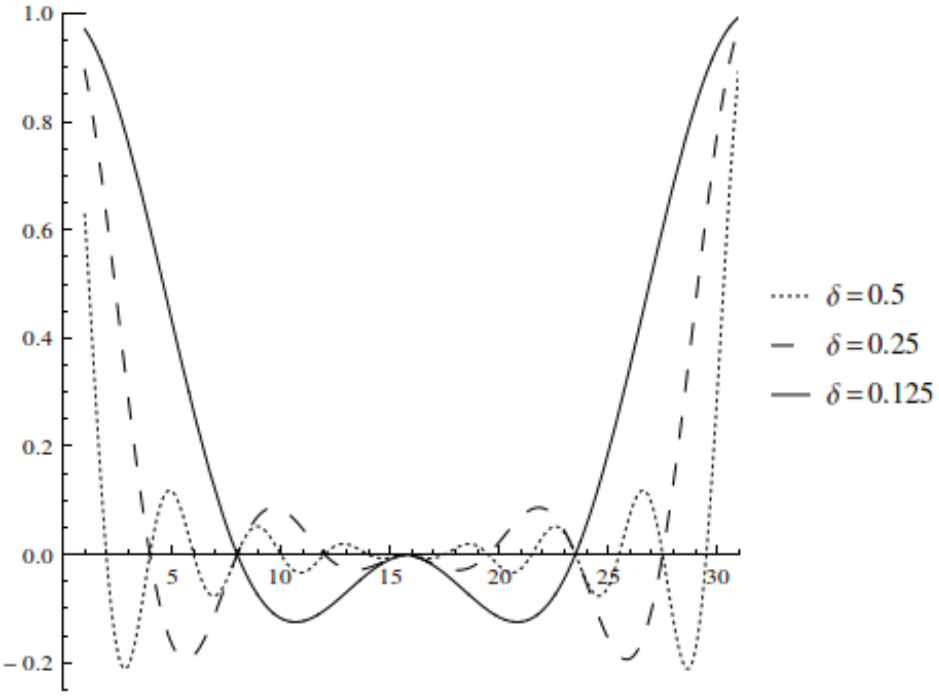

Figure 4.4. Eigenvalues of the iteration matrix $R_{\mathtt{D}}^{p}$ for $\delta = 0.5, 0.25, 0.125$ when $n = 33$. We assume that eigenvalues are continuous in k.

parameters.

Assume that $\lambda_k(A_{\mathtt{a}}^s)$, $\lambda_k(A_{\mathtt{D}}^s)$, $\lambda_k(R_{\mathtt{a}}^w)$ and $\lambda_k(R_{\mathtt{D}}^w)$ are continuous in k. It is easy to see that critical points of $\lambda_k(R_{\mathtt{a}}^w)$ and $\lambda_k(R_{\mathtt{D}}^w)$ do not change with respect to w and are same with of $\lambda_k(A_{\mathtt{a}}^s)$ and $\lambda_k(A_{\mathtt{D}}^s)$, respectively. After this point, we continue with the matrix $A_{\mathtt{a}}^s$. Recall that modes with wavenumbers in the range $\frac{n-1}{4} < k \leq \frac{3(n-1)}{4}$ are oscillatory modes. Let

$$\lambda_k^*(A_{\mathtt{a}}^s) = \max_{\frac{n-1}{4}<k\leq\frac{3(n-1)}{4}} \{\lambda_k(A_{\mathtt{a}}^s)\}, \qquad \lambda_k^{**}(A_{\mathtt{a}}^s) = \min_{\frac{n-1}{4}<k\leq\frac{3(n-1)}{4}} \{\lambda_k(A_{\mathtt{a}}^s)\}.$$

In order to find the optimal value of w, we set $\lambda_k^*(R_{\mathtt{a}}^w) = -\lambda_k^{**}(R_{\mathtt{a}}^w)$, i.e.,

$$1 - \frac{w}{2\delta - h}\lambda_k^*(A_{\mathtt{a}}^s) = -1 + \frac{w}{2\delta - h}\lambda_k^{**}(A_{\mathtt{a}}^s).$$

Solving the above equation for w, we get

$$w = \frac{2(2\delta - h)}{\lambda_k^*(A_{\mathtt{a}}^s) + \lambda_k^{**}(A_{\mathtt{a}}^s)}.$$

Main diagonal of the matrix $A_{\mathtt{D}}^s$ is not constant but if we choose $D_{\mathtt{D}} = (2\delta - h)I$ in the following splitting

$$A_{\mathtt{D}}^s = D_{\mathtt{D}} + L_{\mathtt{D}} + U_{\mathtt{D}}$$

where $L_{\mathtt{D}}$ is lower triangular and $U_{\mathtt{D}}$ is upper triangular, then everything which is done for $A_{\mathtt{a}}^s$ works for $A_{\mathtt{D}}^s$. We show the eigenvalues of $R_{\mathtt{a}}^w$ and $R_{\mathtt{D}}^w$ in Figure 4.5 for different values of δ ($\delta = 0.5, 0.25, 0.125$) when $n = 33$. We give the corresponding values of w on the graphs. Graphs show that the algorithm we propose is working properly.

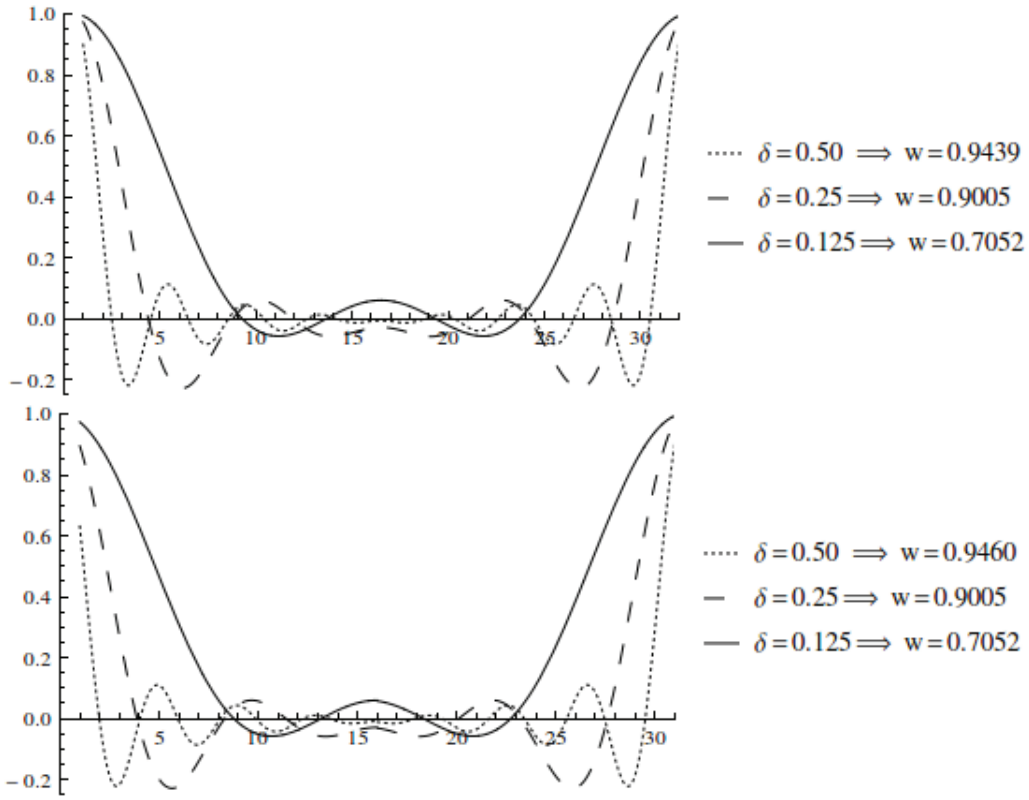

Figure 4.5. Eigenvalues of the iteration matrix $R_{\mathtt{a}}^w$ (above) and $R_{\mathtt{D}}^w$ (below) for $\delta = 0.5, 0.25, 0.125$ when $n = 33$. We assume that eigenvalues are continuous in k.

4.2.3. Numerical Test 1

Now, we are in a position to make comparisons between two strategies. We only consider the matrix $A^s_{\mathtt{D}}$. The results for $A^s_{\mathtt{a}}$ are similar. The smoother in the multigrid context has only the purpose to enable a fast multigrid convergence. We do our comparisons based on this fact. To carry out this, we set up the following two-grid iteration matrix and calculate the spectral norms

$$R^{TG}_{\mathtt{D}} = (I - I^h_{2h}(A^{s,2h}_{\mathtt{D}})^{-1} I^{2h}_h A^{s,h}_{\mathtt{D}}) R^p_{\mathtt{D}}.$$

In the above definition, the prolongation (interpolation) operator I^h_{2h} is the linear interpolation which is given in matrix form as

$$I^h_{2h} = \frac{1}{2} \begin{bmatrix} 1 & & & & \\ 2 & & & & \\ 1 & 1 & & & \\ & 2 & & & \\ & 1 & 1 & & \\ & & 2 & \ddots & \\ & & 1 & \ddots & \\ & & & & 1 \\ & & & & 2 \\ & & & & 1 \end{bmatrix} \in \mathbb{R}^{(n-2)\times(n-3)/2}$$

and restriction operator I^{2h}_h is the transpose of the prolongation operator

$$I^{2h}_h = \left(I^h_{2h}\right)^T.$$

Coarse grid matrix $A^{s,2h}_{\mathtt{D}}$ is defined by Galerkin projection

$$A^{s,2h}_{\mathtt{D}} = I^{2h}_h A^{s,h}_{\mathtt{D}} I^h_{2h}.$$

In Table 4.1, we report spectral norms of the matrix $R_{\mathtt{D}}^{TG}$ for varying mesh size $h = 2^l, l = 3, ...9.$ when $\delta = 2^{-2}$. Although as $h \to 0$ the convergence rates for the two strategies seem equivalent, for bigger mesh sizes convergence rates for the second strategy are smaller. In any case, the second strategy is not worse than the first one. In Table 4.2, we report spectral norms of the matrix $R_{\mathtt{D}}^{TG}$ for varying mesh size $h = 2^{-l}, l = 3, ...9.$ when the ratio δ/h is fixed i.e, $\delta/h = 2$. This situation may occur when δ is very small. In this case, for all values of h convergence rates for the second strategy are smaller than the first one's.

Table 4.1. Spectral norm of two-grid iteration matrix $R_{\mathtt{D}}^{TG}$ for the two strategies for varying h when $\delta = 2^{-2}$.

	$\|\|R_{\mathtt{D}}^{TG}\|\|_2$ (the first strategy)	$\|\|R_{\mathtt{D}}^{TG}\|\|_2$ (the second strategy)
$h = 2^{-3}$	0.5000	0.3951
$h = 2^{-3}$	0.1727	0.1423
$h = 2^{-4}$	0.1083	0.1054
$h = 2^{-5}$	0.0603	0.0597
$h = 2^{-6}$	0.0310	0.0309
$h = 2^{-7}$	0.0156	0.0156
$h = 2^{-8}$	0.0078	0.0078
$h = 2^{-9}$	0.0039	0.0039
$h = 2^{-10}$	0.0020	0.0020

Table 4.2. Spectral norm of two-grid iteration matrix $R_{\mathtt{D}}^{TG}$ for the two strategies when $\delta/h = 2$.

	$\|\|R_{\mathtt{D}}^{TG}\|\|_2$ (the first strategy)	$\|\|R_{\mathtt{D}}^{TG}\|\|_2$ (the second strategy)
$h = 2^{-3}$	0.1549	0.1360
$h = 2^{-3}$	0.1727	0.1423
$h = 2^{-4}$	0.1727	0.1443
$h = 2^{-5}$	0.1727	0.1450
$h = 2^{-6}$	0.1729	0.1451
$h = 2^{-7}$	0.1729	0.1451
$h = 2^{-8}$	0.1729	0.1451
$h = 2^{-9}$	0.1729	0.1451
$h = 2^{-10}$	0.1729	0.1451

4.3. Convergence Analyses

4.3.1. Two-Grid Method

We consider a grid with size h and the corresponding linear system of equations

$$A_{\mathtt{D}}^{s,h}u^h = f^h.$$

The eigenvalues and the eigenvectors of $A_{\mathtt{D}}^s$ are more involved than of $A_{\mathtt{a}}^s$. The analysis we will do can be easily applied to the system $A_{\mathtt{a}}^{s,h}u^h = f^h$ by following the same steps. However, due to the Toeplitz property of $A_{\mathtt{a}}^s$, it may have some superiority in operation count when applying multigrid method.

We consider the prolongation (interpolation), restriction operators and coarse grid matrix defined before in Section 4.2.3. We give the algorithm of two-grid method in Algorithm 1. We apply only one pre-smoothing step and do not apply post-smoothing.

`Step 1`**:** Smooth $A_{\mathtt{D}}^{s,h}\mathbf{u}^h = \mathbf{f}^h$ with Picards' iteration with one step on Ω^h to get an approximation $\mathbf{v}^h$ to $\mathbf{u}^h$.

`Step 2`**:** Compute the residual $\mathbf{r}^h = \mathbf{f}^h - A_{\mathtt{D}}^{s,h}\mathbf{v}^h$.

`Step 3`**:** Restrict the residual $\mathbf{r}^h$ to the coarse grid Ω^{2h} using the restriction operator I_h^{2h}.

`Step 4`**:** Solve the coarse grid equation

$$A_{\mathtt{D}}^{s,2h}\mathbf{e}^{2h} = I_h^{2h}(\mathbf{r}^h)$$

on Ω^{2h}.

`Step 5`**:** Prolongate $\mathbf{e}^{2h}$ to Ω^h using the prolongation operator I_{2h}^h and update $\mathbf{v}^h := \mathbf{v}^h + I_{2h}^h(\mathbf{e}^{2h})$.

Algorithm 1: Two-Grid method without post-smoothing

4.3.2. Convergence Analysis of the Two-Grid Method

It is well known that a necessary and sufficient condition for the convergence of the two-grid method is that spectral radius of the iteration matrix is less than 1. But, even for simple model problems, finding the spectral radius of the iteration matrix is rather difficult. In order to find upper bound for the spectral radius, generally norm estimates are used. This approach may cause loss of some information and may give rough estimate for the spectral radius.

In order to show the roles of δ and h in convergence, we aim to find eigenvalues of the iteration matrix, explicitly. The iteration matrix is given by

$$R_{\mathtt{D}}^{TG} = (I - I_{2h}^{h}(A_{\mathtt{D}}^{s,2h})^{-1} I_{h}^{2h} A_{\mathtt{D}}^{s,h}) R_{\mathtt{D}}^{p}.$$

In the above equation, $R_{\mathtt{D}}^{p}$ stands for the iteration matrix of Picards' iteration with one step. We have already analyzed its spectral properties in Section 4.2. To find the eigenvalues of $R_{\mathtt{D}}^{TG}$, we start examining the properties of the restriction and the prolongation operators defined before. One can show that the prolongation operator satisfies

$$I_{2h}^{h} v_k^{2h} = \cos^2(\frac{k\pi}{n-1}) v_k^h - \sin^2(\frac{k\pi}{n-1}) v_{\frac{n-1}{2}-k}^h \quad \text{for} \quad 1 \le k < \frac{n-1}{4}$$

and

$$I_{2h}^{h} v_k^{2h} = \cos^2\left(\frac{(k+1/2)\pi}{n-1}\right) v_k^h - \sin^2\left(\frac{(k+1/2)\pi}{n-1}\right) v_{\frac{3n-5}{2}-k}^h$$

for $\frac{n-1}{2} \le k \le \frac{3(n-1)}{4}$. Notice that, $v_k^{2h} = -v_{n-2-k}^{2h}$ for $\frac{n-1}{2} \le k \le \frac{3(n-1)}{4}$.

The restriction operator we consider which is the transpose of the prolongation operator has the following properties

$$I_{h}^{2h} v_k^h = 2\cos^2(\frac{k\pi}{n-1}) v_k^{2h} \quad \text{for} \quad 1 \le k < \frac{n-1}{2}$$

and

$$I_h^{2h} v^h_{\frac{n-1}{2}-k} = -2\sin^2(\frac{k\pi}{n-1}) v_k^{2h} \quad 1 \le k < \frac{n-1}{2}$$

in the first half of the spectrum. In the second half of the spectrum, it satisfies

$$I_h^{2h} v_k^h = 2\cos^2\left(\frac{(k+1/2)\pi}{n-1}\right) v_k^{2h} \quad \text{for} \quad \frac{n-1}{2} \le k \le n-2$$

and

$$I_h^{2h} v^h_{\frac{3n-5}{2}} = -2\sin^2\left(\frac{(k+1/2)\pi}{n-1}\right) v_k^{2h} \quad \frac{n-1}{2} \le k \le n-2.$$

As we said before, the coarse grid matrix is obtained by Galerkin projection. That is,

$$A_{\mathtt{D}}^{s,2h} = I_h^{2h} A_{\mathtt{D}}^{s,h} I_{2h}^h.$$

Using this definition and properties of the restriction and prolongation operators mentioned above, we arrive at

$$A_{\mathtt{D}}^{s,2h} v_{i_k}^{2h} = \left(2\lambda_k(A_{\mathtt{D}}^{s,h})\cos^4(\frac{k\pi}{n-1}) + 2\lambda_{\frac{n-1}{2}-k}(A_{\mathtt{D}}^{s,h})\sin^4(\frac{k\pi}{n-1})\right) v_{i_k}^{2h}$$

for $1 \le k < \frac{n-1}{2}$ and

$$A_{\mathtt{D}}^{s,2h} v_{i_k}^{2h} = \left(2\lambda_k(A_{\mathtt{D}}^{s,h})\cos^4\left(\frac{(k+1/2)\pi}{n-1}\right) + 2\lambda_{\frac{3n-5}{2}-k}(A_{\mathtt{D}}^{s,h})\sin^4\left(\frac{(k+1/2)\pi}{n-1}\right)\right) v_{i_k}^{2h}$$

for $\frac{n-1}{2} \le k \le n-2$. Here,

$$\lambda_{\frac{n-1}{2}-k}(A_{\mathtt{D}}^{s,h}) = 2\delta + h\frac{\sin(k\pi\delta)\sin(k\pi h)}{2\cos^2(\frac{k\pi h}{2})}, \qquad 1 \le k < \frac{n-1}{2} \tag{4.13}$$

and

$$\lambda_{\frac{3n-5}{2}-k}(A_{\mathtt{D}}^{s,h}) = 2\delta + h\frac{\sin\left(\left(k+\frac{1}{2}\right)\pi\delta\right)\sin\left(\left(k+\frac{1}{2}\right)\pi h\right)}{2\cos^2\left(\frac{\left(k+\frac{1}{2}\right)\pi h}{2}\right)}, \qquad \frac{n-1}{2} \leq k \leq n-2. \tag{4.14}$$

From the definition of $\lambda_k(A_{\mathtt{D}}^{s,h})$ in (4.10), it is easy to show (4.13) and (4.14).

The iteration matrix $R_{\mathtt{D}}^{TG}$ is not symmetric. So, to find $\rho(R_{\mathtt{D}}^{TG})$, we need the eigenvalues of of the matrix $R_{\mathtt{D}}^{TG^T}R_{\mathtt{D}}^{TG}$. Nevertheless, we give the eigenvectors and the eigenvalues of the matrix $R_{\mathtt{D}}^{TG}$ in case it may shed some light for future works. Eigenvectors of the iteration matrix $R_{\mathtt{D}}^{TG}$ are of the form

$$\mathbf{v}_{i_k}^{TG} = \mathbf{v}_k - \mathbf{v}_{\frac{n-1}{2}-k} \quad \text{for} \quad 1 \leq k < \frac{n-1}{4}$$

and

$$\mathbf{v}_{i_k}^{TG} = \mathbf{v}_k - \mathbf{v}_{\frac{3n-5}{2}-k} \quad \text{for} \quad \frac{n-1}{2} \leq k \leq \frac{3(n-1)}{4}.$$

Their corresponding eigenvalues are all 0. Furthermore, we have the following eigenvectors

$$\mathbf{v}_{i_k}^{TG} = \mathbf{v}_k + c\mathbf{v}_{\frac{n-1}{2}-k} \quad \text{for} \quad 1 \leq k \leq \frac{n-1}{4}$$

and

$$\mathbf{v}_{i_k}^{TG} = \mathbf{v}_k + c\mathbf{v}_{\frac{3n-5}{2}-k} \quad \text{for} \quad \frac{n-1}{2} \leq k \leq \frac{3(n-1)}{4}$$

where

$$c = \frac{\cos^2(\frac{k\pi}{n-1})\lambda_k(A_{\mathtt{D}}^{s,h})}{\sin^2(\frac{k\pi}{n-1})\lambda_{\frac{n-1}{2}-k}(A_{\mathtt{D}}^{s,h})} \quad \text{for} \quad 1 \leq k \leq \frac{n-1}{4}$$

and

$$c = \frac{\cos^2\left(\frac{(k+1/2)\pi}{n-1}\right)\lambda_k(A_{\mathtt{D}}^{s,h})}{\sin^2\left(\frac{(k+1/2)\pi}{n-1}\right)\lambda_{\frac{3n-5}{2}-k}(A_{\mathtt{D}}^{s,h})} \quad \text{for} \quad \frac{n-1}{2} \leq k \leq \frac{3(n-1)}{4}.$$

The corresponding nonzero eigenvalues are found as

$$\lambda_k(R_{\mathtt{D}}^{TG}) = 1 - \frac{\lambda_k(A_{\mathtt{D}}^{s,h})\lambda_{\frac{n-1}{2}-k}(A_{\mathtt{D}}^{s,h})\left(\cos^4(\frac{k\pi}{n-1}) + \sin^4(\frac{k\pi}{n-1})\right)}{\delta\lambda_k(A_{\mathtt{D}}^{s,2h})}$$

for $1 \leq k \leq \frac{n-1}{4}$ and

$$\lambda_k(R_{\mathtt{D}}^{TG}) = 1 - \frac{\lambda_k(A_{\mathtt{D}}^{s,h})\lambda_{\frac{3n-5}{2}-k}(A_{\mathtt{D}}^{s,h})\left(\cos^4\left(\frac{(k+1/2)\pi}{n-1}\right) + \sin^4\left(\frac{(k+1/2)\pi}{n-1}\right)\right)}{\delta\lambda_k(A_{\mathtt{D}}^{s,2h})}$$

for $\frac{n-1}{2} \leq k \leq \frac{3(n-1)}{4}$. In finding the above eigenvalues, the equalities in Lemma 4.3.1 are used.

Lemma 4.3.1 *The following equalities hold.*

$$\sin^2\left(\frac{k\pi}{n-1}\right)\lambda_k(A_{\mathtt{D}}^{s,h}) + \cos^2\left(\frac{k\pi}{n-1}\right)\lambda_{\frac{n-1}{2}-k}(A_{\mathtt{D}}^{s,h}) = 2\delta,$$

for $1 \leq k < \frac{n-1}{2}$ *and*

$$\sin^2\left(\frac{(k+1/2)\pi}{n-1}\right)\lambda_k(A_{\mathtt{D}}^{s,h}) + \cos^2\left(\frac{(k+1/2)\pi}{n-1}\right)\lambda_{\frac{3n-5}{2}-k}(A_{\mathtt{D}}^{s,h}) = 2\delta,$$

for $\frac{n-1}{2} \leq k \leq n-2$.

Proof The proofs follow from the definitions of $\lambda_k(A_{\mathtt{D}}^{s,h})$, $\lambda_{\frac{n-1}{2}-k}(A_{\mathtt{D}}^{s,h})$ and $\lambda_{\frac{3n-5}{2}-k}(A_{\mathtt{D}}^{s,h})$ given in (4.10), (4.13) and (4.14), respectively.

□

Since the iteration matrix $R_{\mathtt{D}}^{TG}$ is not symmetric, to find $\rho\left(R_{\mathtt{D}}^{TG}\right)$ or an approximate upper bound to it, we have to find the eigenvalues of the matrix $R_{\mathtt{D}}^{TG,T}R_{\mathtt{D}}^{TG}$ where $R_{\mathtt{D}}^{TG,T}$ is the transpose of the matrix $R_{\mathtt{D}}^{TG}$. Here, just for notational simplicity, we set $R_{\mathtt{D}}^{TG,m} = R_{\mathtt{D}}^{TG,T}R_{\mathtt{D}}^{TG}$. We found that

$$R_{\mathtt{D}}^{TG,m} = R_{\mathtt{D}}^{p}(I - A_{\mathtt{D}}^{s}I_{2h}^{h}(A_{\mathtt{D}}^{s,2h})^{-1}I_{h}^{2h})(I - I_{2h}^{h}(A_{\mathtt{D}}^{s,2h})^{-1}I_{h}^{2h}A_{\mathtt{D}}^{s})R_{\mathtt{D}}^{p}.$$

Eigenvectors of the matrix $R_{\mathtt{D}}^{TG,m}$ are of the form

$$\mathbf{v}_{i_k}^{TG,m} = \mathbf{v}_k - \mathbf{v}_{\frac{n-1}{2}-k} \quad \text{for} \quad 1 \leq k < \frac{n-1}{4}$$

and

$$\mathbf{v}_{i_k}^{TG,m} = \mathbf{v}_k - \mathbf{v}_{\frac{3n-5}{2}-k} \quad \text{for} \quad \frac{n-1}{2} \leq k \leq \frac{3(n-1)}{4}.$$

Their corresponding eigenvalues are all 0. Furthermore, we have the following eigenvectors

$$\mathbf{v}_{i_k}^{TG,m} = \mathbf{v}_k + \mathbf{v}_{\frac{n-1}{2}-k} \quad \text{for} \quad 1 \leq k \leq \frac{n-1}{4}$$

and

$$\mathbf{v}_{i_k}^{TG,m} = \mathbf{v}_k + \mathbf{v}_{\frac{3n-5}{2}-k} \quad \text{for} \quad \frac{n-1}{2} \leq k \leq \frac{3(n-1)}{4}.$$

Their corresponding eigenvalues are found as

$$\lambda_k(R_{\mathtt{D}}^{TG,m}) = \frac{4h^2 l_1(k,\delta,h) h_1(k,\delta,h)}{2\delta^2 g_1(k,\delta,h)} \quad \text{for} \quad 1 < k < \frac{n-1}{4} \tag{4.15}$$

and

$$\lambda_k(R_{\mathtt{D}}^{TG,m}) = \frac{4h^2 l_2(k,\delta,h) h_2(k,\delta,h)}{2\delta^2 g_2(k,\delta,h)} \quad \text{for} \quad \frac{n-1}{2} \leq k \leq \frac{3(n-1)}{4} \tag{4.16}$$

where

$$l_1(k,\delta,h) = \frac{\sin^4(\frac{k\pi}{n-1}) \left(\lambda_k(A_{\mathtt{D}}^s) - 2\delta\right)^2}{h^2}, \tag{4.17}$$

$$h_1(k,\delta,h) = \lambda^2_{\frac{n-1}{2}-k}(A_{\mathtt{D}}^s) \sin^4(\frac{k\pi}{n-1}) + \lambda_k^2(A_{\mathtt{D}}^s) \cos^4(\frac{k\pi}{n-1}), \tag{4.18}$$

$$g_1(k,\delta,h) = 4\left(\lambda_{\frac{n-1}{2}-k}(A_{\mathtt{D}}^s) \sin^4(\frac{k\pi}{n-1}) + \lambda_k(A_{\mathtt{D}}^s) \cos^4(\frac{k\pi}{n-1})\right)^2, \tag{4.19}$$

$$l_2(k,\delta,h) = \frac{\sin^4(\frac{(k+1/2)\pi}{n-1}) \left(\lambda_k(A_{\mathtt{D}}^s) - 2\delta\right)^2}{h^2}, \tag{4.20}$$

$$h_2(k,\delta,h) = \lambda^2_{\frac{n-1}{2}-k}(A_{\mathtt{D}}^s) \sin^4\left(\frac{(k+1/2)\pi}{n-1}\right) + \lambda_k^2(A_{\mathtt{D}}^s) \cos^4\left(\frac{(k+1/2)\pi}{n-1}\right) \tag{4.21}$$

and

$$g_2(k,\delta,h) = 4\left(\lambda_{\frac{n-1}{2}-k}(A_{\mathtt{D}}^s) \sin^4\left(\frac{(k+1/2)\pi}{n-1}\right) + \lambda_k(A_{\mathtt{D}}^s) \cos^4\left(\frac{(k+1/2)\pi}{n-1}\right)\right)^2. \tag{4.22}$$

In obtaining the above eigenvalues, equalities in Lemma 4.3.1 are used. Now, we try to find upper bounds for eigenvalues given above. We find for the eigenvalues defined in

(4.15). Applying the same steps, the same upper bound can be found for the eigenvalues defined in (4.16). Using Lemma 4.3.2 and Lemma 4.3.3 for $\delta \geq 2h$, we arrive at

$$\lambda_k(R_{\mathtt{D}}^{TG,m}) < \frac{h^2}{2\delta^2}.$$

Since $\delta \geq 2h$, we have

$$\rho\left(R_{\mathtt{D}}^{TG}\right) < \frac{h}{\sqrt{2}\delta} \leq \frac{1}{2\sqrt{2}} = 0.3536.$$

We have found the upper bound for $\delta \geq 2h$, but, our numerical tests showed that the bound is also valid for $\delta = h$. We see that the 2-norm is always less than 1 and strongly depends on the ratio δ/h. The bigger the ratio δ/h is, the smaller the convergence rate becomes. Finally, we numerically verify the upper bound we have found. In Figure 4.6, we present $\rho\left(R_{\mathtt{D}}^{TG}\right)$ and the upper bound $\frac{h}{\sqrt{2}\delta}$ for various δ and h.

Lemma 4.3.2 *The following inequalities hold under the assumption* $\delta/h > 1$.

$$g_1(k,\delta,h) \geq h_1(k,\delta,h), \quad \textit{for} \quad k < \frac{n-1}{2}$$

and

$$g_2(k,\delta,h) \geq h_2(k,\delta,h), \quad \textit{for} \quad k \geq \frac{n-1}{2}$$

where h_1*,* g_1*,* h_2 *and* g_2 *are defined in* (4.18)*,* (4.19)*,* (4.21) *and* (4.22)*, respectively.*

Proof We prove for $k < \frac{n-1}{2}$. For the case $k \geq \frac{n-1}{2}$, the proof follows the same way. It is enough to show that $g_1(k,\delta,h) - h_1(k,\delta,h) \geq 0$. Using trigonometric identities we get

$$g_1(k,\delta,h) - h_1(k,\delta,h) = \tfrac{1}{2}(13\delta^2 + 10\delta^2\cos(2hk\pi) + \delta^2\cos(4hk\pi)$$

$$+4\delta h\sin(2hk\pi)\sin(\delta k\pi) + \delta h\sin(4hk\pi)\sin(\delta k\pi)$$

$$+h^2\sin^2(hk\pi)\sin^2(\delta k\pi)\cos(2hk\pi)).$$

When $\cos(2hk\pi) = -1$, $\cos(4hk\pi) = 1$. Using the fact that $\delta = dh$, where d is a positive integer greater than 1, we arrive at

$$g_1(k,\delta,h) - h_1(k,\delta,h) \geq \tfrac{1}{2}(13d^2h^2 + d^2h^2 - 10d^2h^2 - 4dh^2 - dh^2 - h^2)$$

$$= \tfrac{h^2}{2}(4d^2 - 5d - 1) > 0.$$

This completes the proof.

□

Lemma 4.3.3 *The following inequalities hold.*

$$l_1(k,\delta,h) \leq \frac{1}{4} \qquad \textit{for} \qquad k < \frac{n-1}{2}$$

and

$$l_2(k,\delta,h) \leq \frac{1}{4} \qquad \textit{for} \qquad k \geq \frac{n-1}{2}.$$

where l_1 and l_2 are defined in (4.17) *and* (4.20)*, respectively.*

Proof From the definitions of l_1 and l_2, it is enough to show that

$$-\frac{1}{2} \leq \frac{\sin^2(\frac{k\pi}{n-1})\,(\lambda_k(A_{\mathsf{D}}^s) - 2\delta)}{h} \leq \frac{1}{2}, \qquad k < \frac{n-1}{2}$$

and

$$-\frac{1}{2} \leq \frac{\sin^2(\frac{(k+1/2)\pi}{n-1})\,(\lambda_k(A_{\mathsf{D}}^s) - 2\delta)}{h} \leq \frac{1}{2} \qquad k \geq \frac{n-1}{2}.$$

Doing simple algebraic manipulations in the expression of $\lambda_k(A_{\mathsf{D}}^s)$ in (4.10), the inequal-

ities are obtained.

□

4.4. Multigrid Iteration

4.4.1. Convergence Analysis

We prove the convergence of γ-cycle for $\gamma \geq 2$. To do this, we study the iteration matrix. The levels of the multigrid hierarchy are numbered by $0, ..., l$, where level 0 is the finest grid. The iteration matrix of the of the multigrid γ-cycle without post-smoothing, is given by

$$\begin{cases} R_l^{MG} = R_l, \qquad l = 1, \\ \\ R_l^{MG} = R_l + I_l^{l-1}(R_{l+1}^{MG})^\gamma A_{l+1}^{-1} I_l^{l+1} A_l R^p, \qquad l \geq 2 \end{cases}$$

where R_l is the iteration matrix of the two-level method on level l and given by

$$R_l = (I - I_{l+1}^l A_{l+1}^{-1} I_l^{l+1}) R^p.$$

We will find an upper bound for the spectral radius of R_l^{MG} by the triangle inequality, i.e.

$$||R_l^{MG}||_2 \leq ||R_l||_2 + ||I_l^{l-1}(R_{l+1}^{MG})^\gamma A_{l+1}^{-1} I_l^{l+1} A_l R^p||_2.$$

We can further majorise the right hand side of the above inequality by the rule for norm of the product of the matrices, i.e.

$$||R_l^{MG}||_2 \leq ||R_l||_2 + ||I_l^{l-1}||_2 ||(R_{l+1}^{MG})||_2^\gamma ||A_{l+1}^{-1} I_l^{l+1} A_l R^p||_2. \tag{4.23}$$

One can prove that $||I_{l+1}^{l}||_2 < 2$. It is clear that $||u_{l+1}||_2 \leq ||I_{l+1}^{l} u_{l+1}||_2$ for all u_{l+1} defined on level $l+1$. Using this, we can majorise the last term in (4.23) as follows;

$$||A_{l+1}^{-1} I_l^{l+1} A_l R^p u_l||_2 \leq ||I_{l+1}^{l} A_{l+1}^{-1} I_l^{l+1} A_l R^p u_l||_2$$

for all u_l. Using the definition of an operator norm, we have

$$||A_{l+1}^{-1} I_l^{l+1} A_l R^p||_2 \leq ||I_{l+1}^{l} A_{l+1}^{-1} I_l^{l+1} A_l R^p||_2 = ||R^p - R_l||_2 \leq ||R^p||_2 + ||R_l||_2$$

We have already proved that $||R^p||_2 < 1$ and $||R_l||_2 < \frac{h}{\sqrt{2}\delta}$. Hence, we get

$$||A_{l+1}^{-1} I_l^{l+1} A_l R^p||_2 < 1 + \frac{h}{\sqrt{2}\delta}.$$

Inserting the upper bounds into the right hand side of inequality (4.23), we arrive at

$$||R_l^{MG}||_2 < \frac{h}{\sqrt{2}\delta} + 2\left(1 + \frac{h}{\sqrt{2}\delta}\right) ||(R_{l+1}^{MG})||_2^{\gamma}.$$

The above inequality is of the recursive form

$$x_1 = \frac{h}{\sqrt{2}\delta}, \qquad x_l < \frac{h}{\sqrt{2}\delta} + 2\left(1 + \frac{h}{\sqrt{2}\delta}\right) x_{l+1}^{\gamma}, \qquad l \geq 2. \tag{4.24}$$

Every iterate of (4.24) is bounded by

$$x_l < \frac{\gamma}{\gamma - 1} \frac{h}{\sqrt{2}\delta} < 1.$$

The proof of above inequality can be done by induction and available in John (2013) at page 43. This proves the convergence of multigrid γ-cycle for $\gamma \geq 2$.

4.4.2. Operation Count

The work of one multigrid iteration is dominated by the multiplication of $A_l u_l$. So, we can neglect the works done by I_{l+1}^{l}, I_{l}^{l+1} and vector additions as stated in (Hackbusch (1985), Section: 16.2.1.2). Hence, the total operation count is $\mathcal{O}(dn)$. Same result also was stated in (Chen and Deng (2017), Sec.: 4.1) for multigrid method applied to the original peridynamic operator.

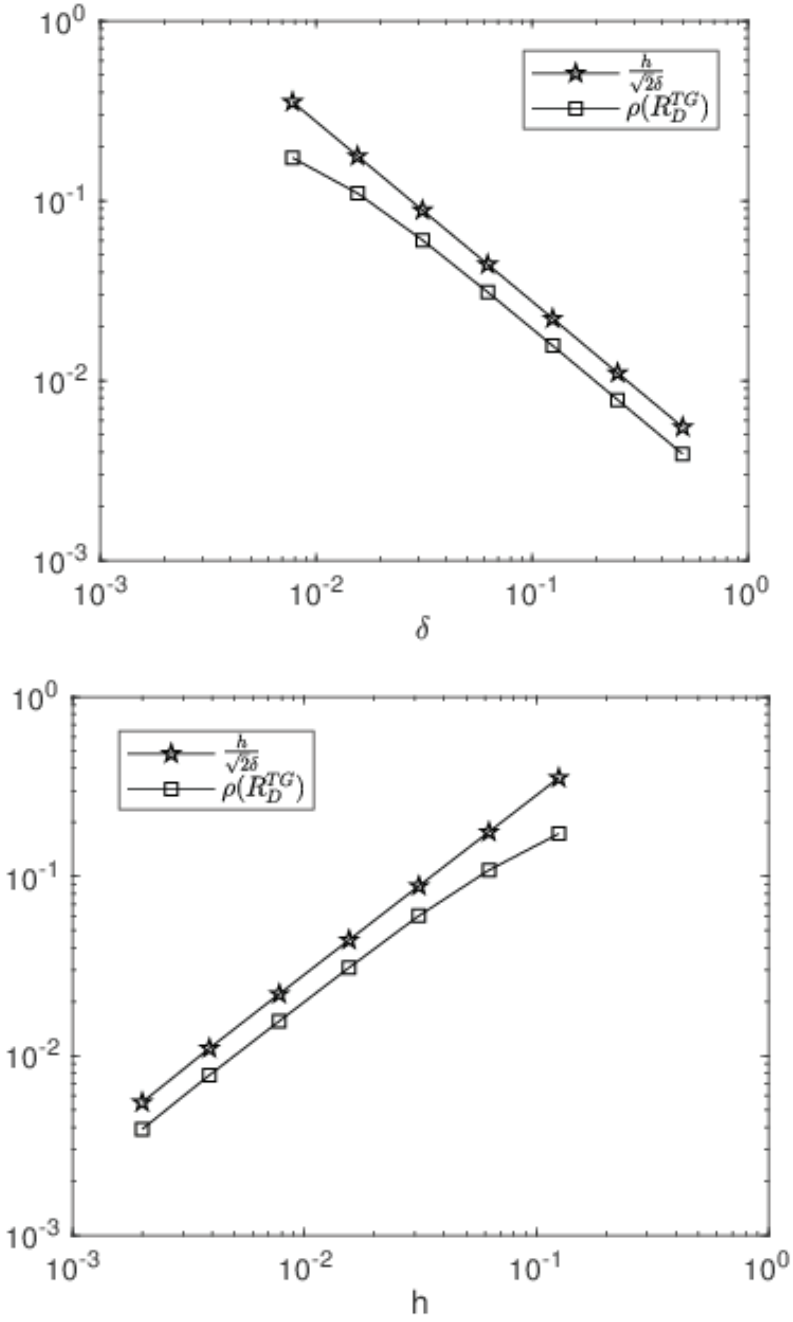

Figure 4.6. $\rho(R_{\mathrm{D}}^{TG})$ and upper bounds for $\rho(R_{\mathrm{D}}^{TG})$. In the figure above , h is set to $h = 0.0039$ and in the figure below, δ is set to $\delta = 0.125$.

CHAPTER 5

CONCLUSION

In this thesis, the numerical solution of nonlocal problems with local boundary conditions is considered. Particularly, we aimed to show the role of the horizon parameter δ in numerical solution. Instead of analyzing system matrices, we analyzed original continuous operators and showed that they have ill-conditioning indicated by δ^{-2}. In numerical tests, we showed that the system matrices of discretized problems have the same ill-conditioning as long as the ratio δ/h is big enough ($\delta \geq 4h$). These results are compatible with the results obtained for original peridynamic operator in Aksoylu and Unlu (2014). So, from conditioning point of view, we can conclude that the novel operators that satisfy local boundary conditions are not far from original peridynamic operator. With the regularity assumption on u and f, we proved rigorously and computationally that the error of Nyström method with trapezoidal rule for Dirichlet and antiperiodic problems is $\mathcal{O}(h^2/\delta^2)$. Here, h^2 comes from numerical integration that is error of trapezoidal rule and $1/\delta^2$ comes from norm of the inverse operators. In order to decrease the error, one can choose either higher order numerical integration or increase the ratio δ/h. We proposed a multigrid method to approximate to the solution of the system of equations. In order to analyze the convergence of the multigrid, we found the spectrum of system matrices in terms of h and δ. We carried out a detailed smoother analysis and our analysis shed some light on working principle of Picards' iteration. We found the spectrum of iteration matrix of two-grid without post-smoothing and thus we obtained a strict upper bound for the spectral norm of the matrix which is $\frac{h}{\sqrt{2}\delta}$. That is, the bigger the ratio $\frac{\delta}{h}$ is, the faster the multigrid convergence is.

In conclusion, the horizon parameter δ plays crucial roles in numerical solutions of nonlocal problems. The problems have ill-conditioning indicated by δ^{-2}. The ratio $\frac{\delta}{h}$ is critical to obtain more accurate and faster approximations. The bigger the ratio $\frac{\delta}{h}$ is, the closer the discrete problem is to the original continuous problem in terms of condition number, the smaller the error is, the faster multigrid convergence is. This should be the case for the original peridynamic problems because our novel operators are not far from it.

REFERENCES

Aksoy, H. G. and E. Senocak (2011). Discontinuous Galerkin method based on peridynamic theory for linear elasticity. *International Journal for Numerical Methods in Engineering 88*, 673–692.

Aksoylu, B., H. R. Beyer, and F. Celiker (2017a). Application and Implementation of Incorporating Local Boundary Conditions into Nonlocal Problems. *Numerical Functional Analysis and Optimization 38*(9), 1077–1114.

Aksoylu, B., H. R. Beyer, and F. Celiker (2017b, aug). Theoretical Foundations of Incorporating Local Boundary Conditions into Nonlocal Problems. *Reports on Mathematical Physics 80*(1), 39–71.

Aksoylu, B. and F. Celiker (2016). Comparison of nonlocal operators utilizing perturbation analysis. In *Lecture Notes in Computational Science and Engineering*, Volume 112, pp. 589–606.

Aksoylu, B. and F. Celiker (2017). Nonlocal problems with local Dirichlet and Neumann boundary conditions. *Journal of Mechanics of Materials and Structures 12*(4), 425–437.

Aksoylu, B., F. Celiker, and O. Kılıçer (2018). Local boundary conditions in nonlocal problems in higher dimensions. *Submitted*.

Aksoylu, B. and A. Kaya (2018a). Conditioning and error analysis of nonlocal operators with local boundary conditions. *Journal of Computational and Applied Mathematics 335*, 1–19.

Aksoylu, B. and A. Kaya (2018b). On a multigrid method for nonlocal problems with local boundary conditions. *Submitted*.

Aksoylu, B. and T. Mengesha (2010). Results on nonlocal boundary value problems. *Numerical Functional Analysis and Optimization 31*(12), 1301–1317.

Aksoylu, B. and M. L. Parks (2011). Variational theory and domain decomposition for nonlocal problems. *Applied Mathematics and Computation 217*(14), 6498–6515.

Aksoylu, B. and Z. Unlu (2014). Conditioning Analysis of Nonlocal Integral Operators in Fractional Sobolev Spaces. *SIAM Journal on Numerical Analysis 52*(2), 653–677.

Alali, B. and R. Lipton (2012). Multiscale dynamics of heterogeneous media in the peridynamic formulation. *Journal of Elasticity 106*(1), 71–103.

Andreu-Vaillo, F., J. M. Mazón, J. D. Rossi, and J. J. Toledo-Melero (2010). *Nonlocal diffusion problems.*, Volume 165.

Atkinson, K. E. (1997). *The Numerical Solution of Integral Equations of the Second Kind*. Cambridge Monographs on Applied and Computational Mathematics. Cambridge University Press.

Beyer, H. R., B. Aksoylu, and F. Celiker (2016). On a class of nonlocal wave equations from applications. *Journal of Mathematical Physics 57*(6).

Böttcher, A. and H. Widom (2007). From Toeplitz Eigenvalues through Green's Kernels to Higher-order Wirtinger-Sobolev Inequalities. In M. A. Dritschel (Ed.), *The Extended Field of Operator Theory*, Basel, pp. 73–87. Birkhäuser Basel.

Bourgain, J., H. Brezis, and P. Mironescu (2001). Another look at Sobolev spaces. *Optimal Control and Partial Differential Equations*, 439–455.

Briggs, W., V. Henson, and S. McCormick (2000). *A Multigrid Tutorial, Second Edition* (Second ed.). Society for Industrial and Applied Mathematics.

Chen, M. and W. Deng (2017). Convergence analysis of a multigrid method for a nonlocal model. *SIAM Journal on Matrix Analysis and Applications 38*(3), 869–890.

Du, Q., M. Gunzburger, R. Lehoucq, and K. Zhou (2012). Analysis and approximation of nonlocal diffusion problems with volume constraints. *SIAM review C*(4), 1–26.

Du, Q. and R. Lipton (2014). Peridynamics, Fracture and Nonlocal Continuum Models. *SIAM news 47*(3).

Du, Q., L. Tian, and X. Zhao (2013). A Convergent Adaptive Finite Element Algorithm for Nonlocal Diffusion and Peridynamic Models. *SIAM Journal on Numerical Analysis 51*(2), 1211–1234.

Du, Q. and K. Zhou (2011). Mathematical analysis for the peridynamic nonlocal continuum theory. *ESAIM: Mathematical Modelling and Numerical Analysis 45*(2), 217–234.

Emmrich, E. and O. Weckner (2007a). Analysis and numerical approximation of an integro-differential equation modeling non-local effects in linear elasticity. *Mathematics and Mechanics of Solids 12*(4), 363–384.

Emmrich, E. and O. Weckner (2007b). On the well-posedness of the linear peridynamic model and its convergence towards the Navier equation of linear elasticity. *Communications in Mathematical Sciences 5*(4), 851–864.

Emmrich, E. and O. Weckner (2007c). The peridynamic equation and its spatial discretisation. *Mathematical Modelling and Analysis 12*(1), 17–27.

Gilboa, G. and S. Osher (2009). Nonlocal Operators with Applications to Image Processing. *Multiscale Modeling & Simulation 7*(3), 1005–1028.

Hackbusch, W. (1979). Multi-grid techniek voor het oplossen van fredholm-integraalvergelijkingen van de tweede soort.

Hackbusch, W. (1981). Die schnelle Auflosung der Fredholmschen Integralgleichung zweiter. *Art. Beitriige Numer Math 9*, 47–62.

Hackbusch, W. (1985). *Multi-Grid Methods and Applications* (1 ed.). Springer-Verlag Berlin Heidelberg.

Hackbusch, W. (2016). *Iterative Solution of Large Sparse Systems of Equations* (2 ed.).

Springer International Publishing.

Hemker, P. and H. Schippers (1981). Multiple grid methods for the solution of Fredholm integral equations of the second kind. *Mathematics of Computation 36*(153), 215–232.

John, V. (2013). Multigrid Methods. Technical report.

Kac, M., W. L. Murdock, and G. Szegö (1953). On the eigenvalues of certain hermitian forms. *Rational Mechanics and Analysis 2*, 767–800.

Kilic, B. (2008). *Peridynamic theory for progressive failure prediction in homogeneous and heterogeneous materials*. Ph. D. thesis.

Kress, R. (1989). *Linear Integral Equations* (1 ed.). Springer-Verlag Berlin Heidelberg.

Madenci, E. and E. Oterkus (2014). *Peridynamic theory and its applications*, Volume 9781461484653.

Mengesha, T. and Q. Du (2014a). Nonlocal constrained value problems for a linear peridynamic navier equation. *Journal of Elasticity 116*(1), 27–51.

Mengesha, T. and Q. Du (2014b). The bond-based peridynamic system with Dirichlet-type volume constraint. *Proceedings of the Royal Society of Edinburgh Section A: Mathematics 144*(1), 161–186.

Ponce, A. C. (2004). An estimate in the spirit of poincaré's inequality. *Journal of the European Mathematical Society 6*(1), 1–15.

Schippers, H. Multi-grid techniques for tbe solution of Fredholm integral equations of the second kind. *In: te Riele 1*, 29–46.

Seleson, P., S. Beneddine, and S. Prudhomme (2013). A force-based coupling scheme for peridynamics and classical elasticity. *Computational Materials Science 66*, 34–49.

Silling, S. A. (2000). Reformulation of elasticity theory for discontinuities and long-range

forces. *Journal of the Mechanics and Physics of Solids 48*(1), 175–209.

Silling, S. A. and R. B. Lehoucq (2008). Convergence of peridynamics to classical elasticity theory. *Journal of Elasticity 93*(1), 13–37.

Silling, S. A. and R. B. Lehoucq (2010). *Peridynamic Theory of Solid Mechanics*, Volume 44.

Tian, X. and Q. Du (2013). Analysis and comparison of different approximations to nonlocal diffusion and linear peridynamic equations. *SIAM Journal on Numerical Analysis 51*(6), 3458–3482.

Web (2014). Introduction to nonlocal equations, Accessed 28 March 2018, https://www.ma.utexas.edu/mediawiki/index.php/Introduction_to_nonlocal_equations.

Zhou, K. and Q. Du (2010). Mathematical and Numerical Analysis of Linear Peridynamic Models with Nonlocal Boundary Conditions. *SIAM Journal on Numerical Analysis 48*(5), 1759–1780.